SOLID SOLUBILITY AND STRENGTHENING EFFECT OF ALUMINUM IN ALPHA ZIRCONIUM

by

Shyam Narayan Tiwari

Thesis submitted in partial fulfillment
of the requirements for the degree of
Master of Science

The Faculty of Graduate Studies and Research
Department of Mechanical Engineering
University of Manitoba
Winnipeg

January 1969

ABSTRACT

In the present investigation the parametric method was used to determine the solvus curve in the zirconium rich region of the Zr-Al system, down to temperatures lower than 700°C. It was found that the empirical relation $\log S \alpha \frac{1}{T^{o}K}$ is obeyed in this system. The lattice parameter 'a' of the α Zr decreased linearly with the aluminum content, while the parameter 'c' changed irregularly. It was observed that the hardness of the Zr-Al solid solutions increased with the increasing aluminum content but it was nearly constant in the two-phase alloys.

Tensile tests were done at room temperature, 300°C and 500°C on polycrystalline specimens of the Zr-Al solid solutions to develop a qualitative understanding of the strengthening behaviour of Al in Zr. A probable explanation has been put forward to explain the high strengthening effect of Al. However, single crystal work based on electron microscopy is necessary to obtain a quantitative understanding of the strengthening behaviour and to substantiate the probable explanation given for it.

ACKNOWLEDGEMENTS

I wish to express my sincere thanks to Dr. K. Tangri, Professor of Metallurgical Sciences, for his continued help and advice throughout this work. I acknowledge the help of my colleague, R. N. Singh, in writing the computer programmes and thank Dr. R. T. Holt for a careful checking of the manuscript.

TABLE OF CONTENTS

FIGURE INDEX

FIGURE INDEX (continued)

TABLE INDEX

SOLID SOLUBILITY AND STRENGTHENING EFFECT OF ALUMINUM IN ALPHA ZIRCONIUM

1 INTRODUCTION AND OBJECTIVES

A comparative study of various binary alloys of zirconium reveals that aluminum is one of the most effective alloying elements in raising the strength of zirconium (figs. 1 and 2)[1].

Apart from the marked strengthening effect of aluminum on zirconium, another noticeable feature of the zirconium-aluminum system is the presence of a 'knee' in its yield stress vs composition curve (figs. 1 and 2). The high strengthening effect observed in the initial stages of aluminum additions followed by very low and again high strengthening on further additions of aluminum suggests that the modes of strengthening in the high and low strengthening regions of the curve are different.

Although no systematic study of the zirconium-aluminum system has been reported, some data resulting from various investigations concerned with the development of zirconium alloys are available[1]. However, it is not possible to draw any valid conclusions regarding the strengthening behaviour of aluminum in the zirconium-aluminum system from these data because of the variations in heat treatment and testing conditions employed by individual investigators.

The strengthening effect of aluminum on zirconium as seen in the different regions of the curve in figs. 1 and 2 may be attributed to the precipitation of a second phase and/or strengthening of the matrix by solution hardening. One of the objectives

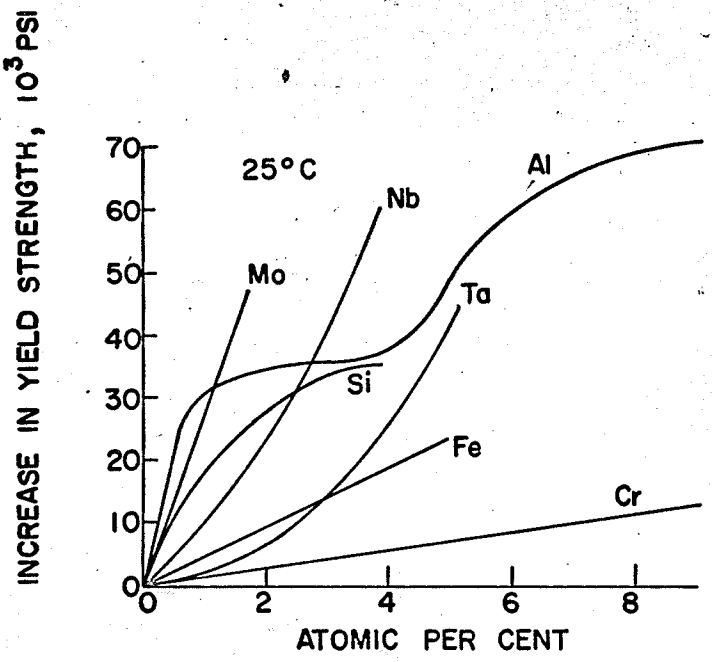

Fig. 1 – Strengthening effect versus per cent element added for various alloying elements in zirconium at 25° C (1)

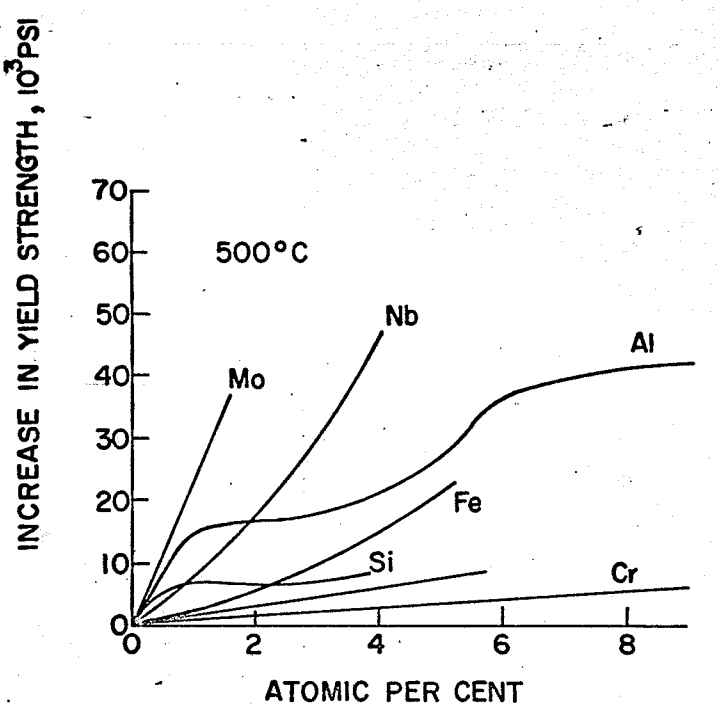

Fig. 2 – Strengthening effect versus per cent element added for various alloying elements in zirconium at 500°C (1)

of the present investigation is to study the contribution of solution strengthening towards the increased strength of alpha zirconium by aluminum additions. In order to separate the effect of precipitation from solution hardening, the solubility limit of aluminum in alpha zirconium should be known at various temperatures, i.e., the solvus for the zirconium-aluminum system should be available.

In the zirconium-aluminum equilibrium diagram, fig. 3[2], (determined by employing metallographic techniques) the solvus has only been determined down to 700°C. There is no information in literature about the solid solubility at temperatures lower than 700°C.

Because grain boundaries act as barriers to the motion of dislocations, they are primary sites of stress concentration and inhomogeneous deformation. Because the orientation of a crystal in an aggregate is, in general, different from its neighbours, each crystal imposes constraints upon its neighbours. Therefore, for fundamental studies on solution strengthening, it is necessary to investigate the behaviour of alloy single crystals. Nevertheless, work on polycrystalline samples, apart from providing technologically useful data, enables one to develop a qualitative understanding of the strengthening mechanisms in a given alloy system.

Thus the two objectives of the present investigation are:

1. the determination of the solid solubility of aluminum in alpha zirconium at temperatures lower than 700°C and
2. the collection of preliminary strength data on polycrystals and the development of a qualitative understanding of the solution hardening mechanism operating in the zirconium-aluminum system.

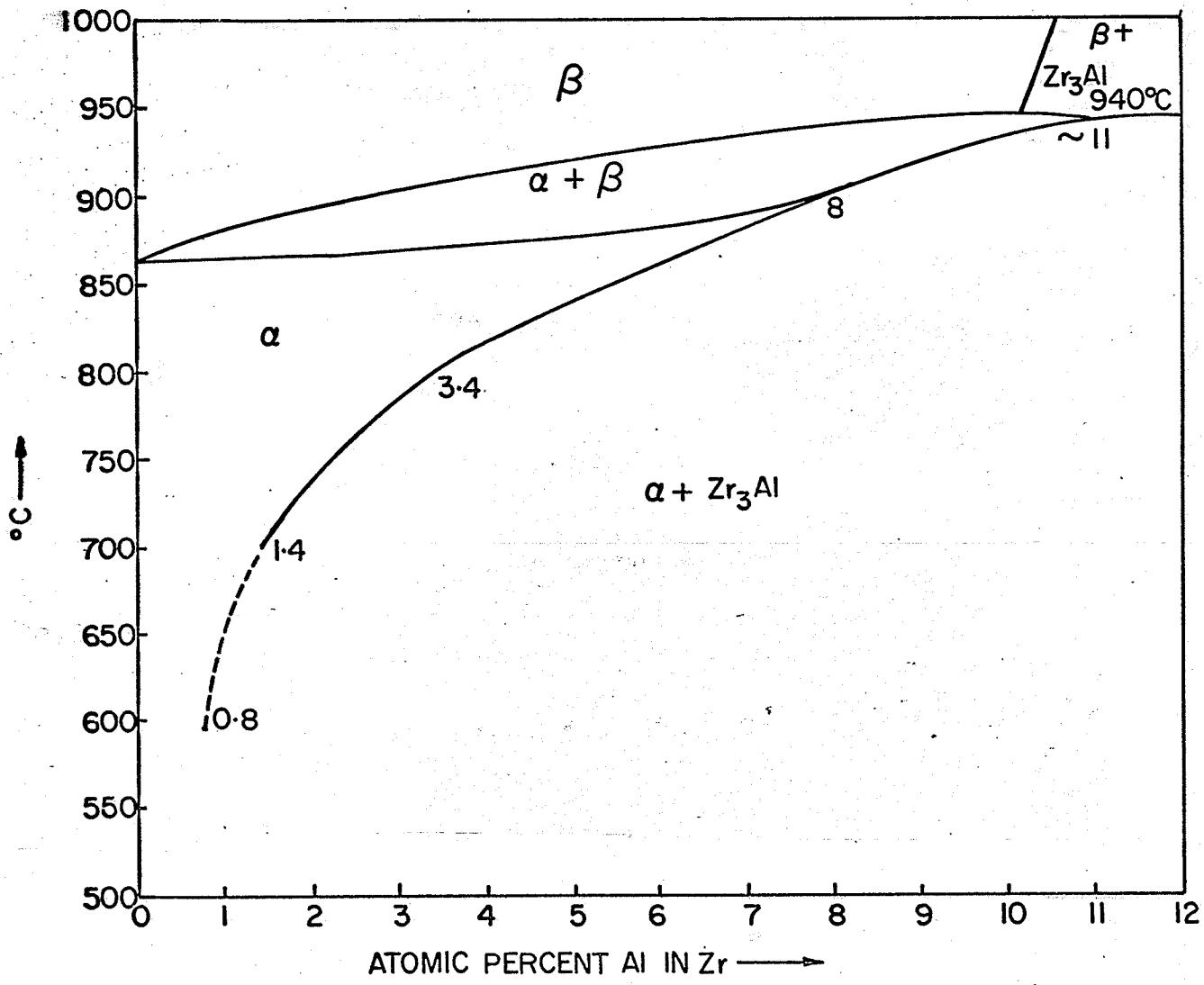

Fig. 3 - Expanded diagram of the zirconium-rich region of the zirconium-aluminum system[2]

2 EXPERIMENTAL PROCEDURE

2.1 Materials and Alloy Preparation

According to the present equilibrium diagram of the zirconium-aluminum system[2] the alpha solid solution region is widest at $\sim 850^{o}C$. As such, it was decided to equilibrate nine alloys at $850^{o}C$, six alloys being in the alpha region and the remaining in the two-phase ($\alpha + Zr_3Al$) region.

The zirconium-aluminum alloys and their chemical analyses were supplied by the Whiteshell Nuclear Research Establishment at Pinawa. For preparing these alloys, reactor grade zirconium and very high purity aluminum (1SF grade) were used. The alloys were argon-arc-melted with a tungsten electrode. The alloy ingots were 2" long, 0.5" in diameter and weighed about 60 gms each.

The chemical analyses of zirconium, aluminum and the alloys are given in tables 1, 2 and 3 respectively.

TABLE 1

Ingot Analysis of Zirconium in ppm

	Top	Bottom		Top	Bottom
Al	< 25	< 25	N	45	28
B	<0.2	<0.2	Ni	< 10	< 10
C	< 40	< 40	O	140	120
Cb	<100	<100	Pb	< 5	< 5
Cd	<0.3	<0.3	Si	< 40	< 40
Co	< 5	< 5	Sn	10	10
Cr	< 10	< 10	Ta	<200	<200
Cu	< 25	< 25	Ti	< 20	< 20
Fe	105	105	V	< 5	< 5
H	7	7	W	< 25	< 25
Hf	125	140	Zn	< 50	< 50
Mg	< 10	< 10	U	<0.5	<0.5
Mn	< 10	< 10			
Mo	< 10	< 10			

TABLE 2

Chemical Analysis of Aluminum

Fe	0.40%
Si	0.25%
Other Impurities	0.15%
Balance Aluminum	

TABLE 3

Chemical Analysis of Zirconium-Aluminum Alloys

Alloy No.	Al W/o	Al A/o	O_2 p.p.m.
1	0.165	0.55517	84
2	0.370	1.23971	332
3	0.593	1.97621	211
4	0.845	2.79981	107
5	1.270	4.16688	217
6	1.610	5.24216	485
7	2.220	7.12800	150
8	2.610	8.30756	72
9	3.250	10.19837	174

2.2 Preparation and Heat Treatment of the Alloy Samples

The alloy ingots were surface ground to remove the oxide layer, thus eliminating the possibility of further oxygen diffusion into the metal during subsequent heat treatments. After grinding, the ingots were chemically cleaned in (45% HNO_3, 45% lactic acid and 10% HF) acid solution and then washed with water and alcohol and dried.

The ingots were given $\sim$ 5-10% reduction by cold rolling (to help in the homogenizing treatment). The ingots were cleaned and wrapped in pure clean zirconium foil ($\sim$ 0.004" thick) and then sealed in a silica tube, after flushing three times with argon and evacuating to a pressure of 1×10^{-5} Torr. The sealed specimens were kept at 1000°C (β region) for 5 hours to homogenize the whole specimen. The specimens were quenched in water by breaking the tube after homogenizing.

Small pieces were cut from the homogenized specimens, marked, cleaned, wrapped and sealed in a silica tube. The sealed specimens

were held at 1000°C for 5 hours after which time the furnace temperature was reduced to ∿ 850°C and then set at 850 ± 1°C. The alloy specimens were equilibrated at 850°C for 120 hours and quenched. The temperature was checked every 12 hours during the equilibrating treatment.

For determining the solid solubility at temperatures lower than 850°C, an alloy in the two-phase (α + Zr_3Al) region was selected. It does not matter which composition is chosen as long as it is in the two-phase (α + Zr_3Al) region because at any temperature only the proportion of α and Zr_3Al changes with composition but the lattice parameters of α remain the same. The parameters of α change with temperature for the same composition of the alloy.

The equilibrating procedure was repeated to equilibrate samples at 700, 600 and 500°C. The equilibrating time at various temperatures (after 5 hours at 1000°C) is given in table 4.

TABLE 4

Equilibrating Time at Various Temperatures

Equilibrating Temperature	Equilibrating Time (hours)	
850°C	120	Water Quenched
700°C	298	-"-
600°C	350	-"-
500°C	500	-"-

2.3 Powder Specimen Preparation and Its X-Ray Diffraction Pattern

After cleaning, the equilibrated alloy samples were deeply filed under CCl_4 by a hard steel file. The samples were then

transferred to another pot containing CCl_4 and were filed again under CCl_4. This procedure minimized the possible oxidation of the surface of the fine particles during their preparation. After producing the requisite amount of powder, the CCl_4 was drained and the powder dried in air. A magnet was run over the dried powder to remove any iron particles produced during the filing operation. This powder was sieved and -200 mesh powder was used as this was considered fine enough to obtain sharp and continuous diffraction lines. This procedure of powder making was repeated on all the alloys.

The fine powders were put in zirconium-foil capsules and sealed in silica tubes. The sealed powder samples were put in furnaces at their respective equilibrating temperatures, i.e., 850°C, 700°C, 600°C and 500°C, to relieve the stresses developed during filing. After one hour the samples were quenched in water without breaking the tube.

The powders were placed in 0.25 mm glass capillary tubes which were then mounted in a 114.6 mm diameter Debye-Scherrer camera. The x-ray film was wrapped in aluminum foil to minimize the scattering effect on the film and to get a sharp diffraction pattern. The camera was loaded by the Straumanis method and the samples were exposed to copper K-alpha radiation for 3.5 hours. During exposure the room temperature was 22 ± 1°C.

Measurements on all the films were made 24 hours after processing them. This step minimized errors which could be caused by the measurement of films not yet completely dry. Distances up to 0.005 cm could be measured with the Phillips film measuring unit.

Cohen's least square method[3] was used to calculate the lattice parameters of the alpha phase.

2.4 Metallographic Examination and the Hardness Measurements

After equilibrating (120 hours at 850°C) and water quenching, the alloys were cold mounted and mechanically polished. After etching with (45% HNO_3, 45% Lactic Acid and 10% HF) acidic solution the samples were examined metallographically. The hardness of these cold mounted samples was determined using the Vickers Pyramid hardness tester with a load of 1 kilogramme.

2.5 Preparation of Polycrystalline Tensile Test Specimens

The zirconium-aluminum alloys selected for the tensile tests are given in table 5.

TABLE 5

Chemical Analysis of the Zirconium-Aluminum Alloys for Tensile Tests

Sample No.	Al W/o	Al A/o	Oxygen ppm	Remarks
1.	0.161	0.5416	423	Argon-arc-melted
2.	0.370	1.2397	332	-"-
3.	0.593	1.9726	211	-"-
4.	0.838	2.7770	209	-"-

The alloy ingots were surface ground and cleaned. They were heated in a neutral salt bath (liquid heat ND1000 from Houghton Co.) maintained at ∿ 875°C and hot rolled to ∿ 1/8" sheets. Two or three passes were given before reheating. The rolled sheets were cleaned in hot water and then in an acidic solution (30% HNO_3, 30% H_2SO_4,

30% H_2O and 10% HF - all by volume). These were cold rolled to ~ 0.045" thick sheets, cleaned and sealed in a silica tube under a pressure of 1 x 10^{-5} Torr. These alloys were equilibrated for 120 hours at 850°C and water quenched.

Tensile test specimens of the size shown in fig. 4 were machined in a standard jig.

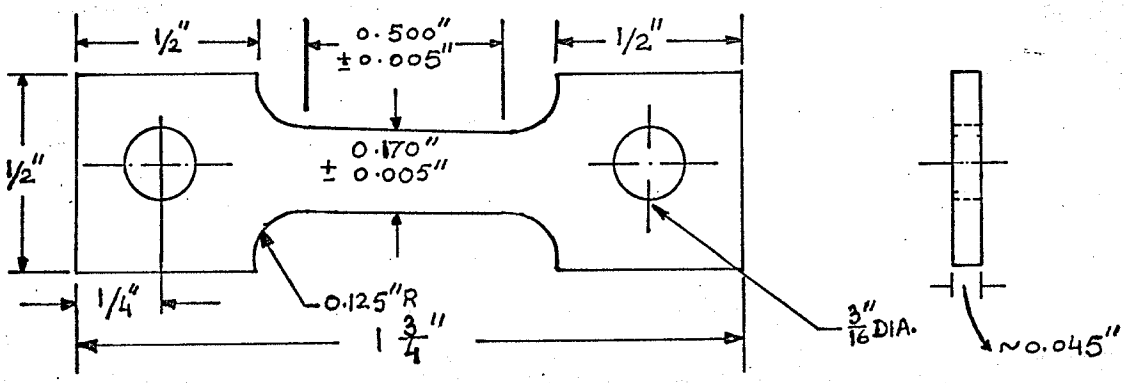

Fig. 4 Tensile Test Specimen

Small pieces from the equilibrated alloys were aged at 300, 500 and 700°C for 10, 20, 40 and 60 minutes and quenched in water. The aged alloys were examined metallographically to determine if precipitation took place in any of the aged specimens. Precipitation was not detected.

2.6 Tensile Tests

A floor model Instron machine was used to perform the tensile tests at room temperature, 300°C and 500°C. Tests at 300 and 500°C were carried out in a dynamic vacuum (10^{-2} Torr.). In all cases duplicate specimens were tested. The crosshead speed was 0.02 inches per minute and the recorder chart speed was set at 2 inches per minute.

The high temperature tests lasted for 50-55 minutes which comprise the time the specimen took to reach the temperature and the time to carry out the test till the fracture occurred.

3 SOLID SOLUBILITY OF ALUMINUM IN ALPHA ZIRCONIUM

3.1 Application of the Alloying Theory

a. Range of favourable size factor for solid solution formation

The atomic diameters of alpha zirconium and aluminum are 3.20 Å and 2.86 Å respectively. This size difference of 10.5% between the solvent and solute atoms is well within the favourable size factor of ±15% as postulated by Hume-Rothery. Thus, on the basis of the size factor alone, considerable solubility of aluminum in alpha zirconium would be expected.

Aluminum crystallizes in the f.c.c. structure, and the curves of Mott and Jones (1937)[6] show that with 3 electrons per atom, there is a moderate overlap across the {200} planes. When the overlap is present the atomic diameter, i.e. the closest distance of approach in pure aluminum is 2.86 Å. Jones[6a] has shown that Brillouin zone overlap produces expansion at this lattice in the same direction as that of the overlap. In aluminum alloy structures where no overlap occurs the atomic diameter of aluminum is 2.70-2.80 Å.

Thus, the size factor is 15.5% rather than 10.5% if the atomic diameter of aluminum is taken as 2.70 Å. This is less favourable to extensive solid solution formation.

b. Electrochemical nature and polarizability

Since zirconium is strongly electropositive (electronegativity of zirconium is 1.6), many of the elements which on size factor grounds alone might form extensive solid solutions will tend to form stable intermetallic compounds instead. This is the behaviour

to be expected with electronegative and weakly eletropositive elements. Aluminum which has an electronegativity of 1.5, which is close to 1.6, will have a lesser tendency to form compounds than solid solutions. But it is known from the zirconium-aluminum equilibrium diagram that compounds are formed and the solid solubility of aluminum in alpha zirconium is restricted.

Although polarizability usually does not play a significant role in intermetallic compounds, it should be noted that the polarizability of zirconium is about twice that of titanium. From this point of view, zirconium will show a stronger tendency to compound formation than titanium. This is revealed in the relative solid solubilities of aluminum in alpha titanium and alpha zirconium, whereas alpha titanium has an extensive solid solution (max. solid solubility over 40 A/o), α zirconium has restricted area of solid solution (maximum $\sim$ 10 A/o).

c. Relative valency effect

A metal of higher valency is more likely to dissolve to a large extent in one of lower valency than vice versa. This rule is a general one only for univalent solvent metals but not so general for solvent metals of higher valencies.

Since the stability of a compound increases with the valence of the solute, electronegativity and size being constant, it would be expected that aluminum which is a trivalent element will have a limited solid solution range in alpha zirconium.

Thus, it would seem that size factor and electrochemical factors are relatively unimportant in determining the extent of solid

solution of aluminum in zirconium and that the electron concentration plays a more important role than the above factors.

3.2 Methods for Determining the Solvus Curve

1. Microscopical method - The great advantage of the microscopical method is that it enables a relatively large area to be examined so that evidence of uneven composition is readily obtained. Chemical analysis can then be carried out on the exact specimen which has been viewed microscopically, and in this way there is a satisfactory control of the composition of the specimen. If the crystals present are not too small, and the alloys are such that phases do not decompose on quenching, it is quite easy to detect one percent of a phase present in a two phase alloy.

In determination of a solvus curve where the extent of the α phase diminishes with the falling temperature, it is common practice to homogenize specimens by annealing at a high temperature, and then to reanneal at a lower temperature, after which microscopical examination is used to determine if precipitation of the second phase has occurred. In every alloy there is a temperature below which the growth of the precipitated particles to an observable size is so slow that extremely long times of annealing are required. In such cases there is always a danger that alloys examined microscopically may be classed as homogeneous when they would really contain two or more phases under equilibrium conditions.

2. X-ray methods[4] -

a. Disappearing phase method - This method is based on the 'lever' law. Thus with reference to figure 5 the relative proportion

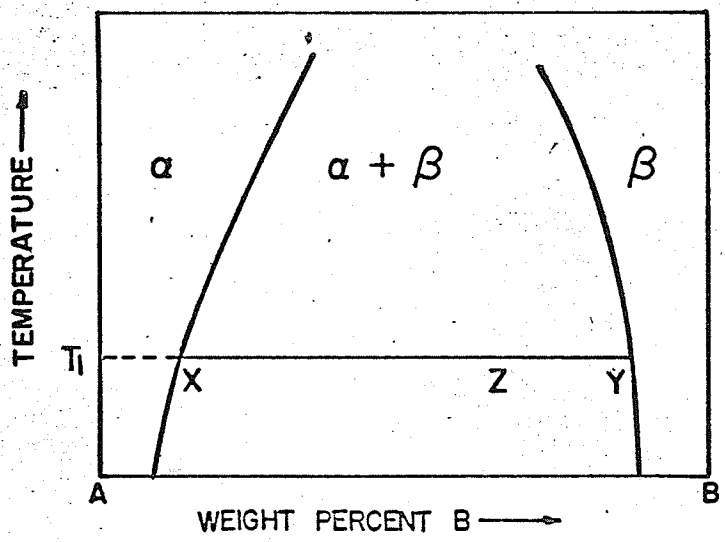

Fig. 5 The relative proportion of α and β in an alloy of composition Z at temperature T_1.

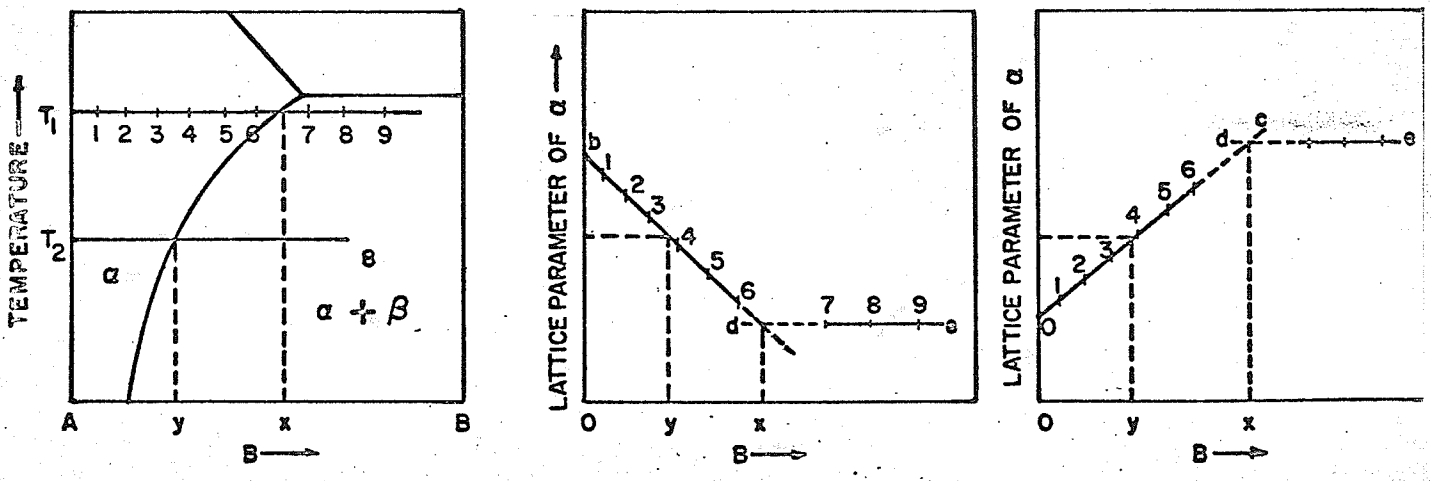

Fig. 6 Schematic representation of the parameter method

of α and β in an alloy of composition Z at temperature T_1 is given by the relative lengths of the line ZY and ZX

$$W_\alpha : W_\beta = ZY : ZX.$$

Thus we see the weight fraction of β in the alloy varies linearly with composition from 0 at point X to 1 at point Y. The intensity of any diffraction line from the β phase also varies from zero at X to a maximum at Y, (but the variation with weight percent is not generally linear). This variation may be used to locate the point X. A series of alloys in the two-phase region is brought to equilibrium at temperature T_1 and quenched. From diffraction patterns made at room temperature, the ratio of the intensity I_β of a prominent line of β phase to the intensity I_α of a prominent line of the α phase is plotted as a function of weight percent B. The composition at which the ration I_β/I_α extrapolates to zero is taken as the point X. Other points on the solvus curve are located in similar ways from alloys quenched from other temperatures.

b. Parametric method - This method depends upon the fact that the lattice-parameter of a solid solution generally changes with composition up to the saturation limit, and then remains constant beyond that point, figure 6. This method was used in the present investigation.

For a given accuracy of lattice parameter measurement, the accuracy with which the solvus can be located depends markedly on the slope of the parameter-composition curve. If changes in the composition of the solid solution produce very small changes in

parameter, then the composition as determined from the parameter will be subject to considerable error and so will the location of the solvus. However, if the curve is steep, just the opposite is true.

In most cases, the parametric method is more accurate than the disappearing-phase method (whether based on x-ray measurements or miscroscopic examination) in the determination of solvus curves at low temperatures, as both may fail to disclose the presence of small amounts of a second phase, although for different reasons. When this occurs, the disappearing-phase method always results in a measured extent of solubility higher than the actual extent. But the parametric method, since it is based on the measurements made on the phase whose range of solubility is being determined (α), is not influenced by any property of the second phase (β).

The advantage of the parametric measurements method is that powder specimens can be used without any concern of reducing the proportion of one phase, (usually the brittle phase) after sieving and thus in turn affecting the intensity of that phase in the disappearing-phase method. Thus the parametric method is suitable for alloys having phase which differ greatly in brittleness.

On comparing the three methods discussed, it is clear that the parametric method is superior to the other two methods and in the present case is very suitable to the Zr-Al system as the two phases (α and Zr_3Al) differ greatly in hardness (the hardness of zirconium is $\sim$ 100 VPN and that of Zr_3Al is 390-445 VPN). Moreover, the lattice parameters of the α phase of Zr-Al alloys in the single

phase region could be used in relating the change in the lattice parameters to the strengthening effect of Al on α Zr which is one of the objectives of the present investigation.

3.3 Results and Discussion

3.3.1 Lattice parameters of the zirconium-aluminum solid solutions

Lattice parameters of the alpha phase of the alloys equilibrated at 850°C are given in table 6.

TABLE 6

Lattice Parameters of the Alloys Equilibrated at 850°C

Sample No.	Al		Lattice Parameter	Lattice Parameter	
	W/o	A/o	a Å	c Å	c/a
1	0.165	0.552	3.23091	5.14194	1.59149
2	0.370	1.240	3.22813	5.13017	1.58921
3	0.593	1.976	3.22731	5.13406	1.59082
4	0.845	2.800	3.22117	5.13645	1.59459
5	1.270	4.167	3.21397	5.13103	1.59648
6	1.610	5.242	3.21034	5.12469	1.59630
7	2.220	7.128	3.20668	5.12581	1.59848
8	2.610	8.308	3.20666	5.12123	1.59706
9	3.250	10.198	3.20772	5.12473	1.59762

Compositions and lattice parameters of the alpha phase of the alloys equilibrated at 700°C for 298 hours, at 600°C for 350 hours

and at 500°C for 500 hours are shown in table 7.

The decrease in lattice parameter "a" of the alpha solid solution, figure 7, is very nearly linear with aluminum content and thus obeys the Vegard's law at least for "a". The change in "a" with aluminum content can be expressed by the relation

$$a = 3.2332 - 0.0044\,x$$

where a = lattice parameter of the alpha phase in Å

x = aluminum content in A/o.

TABLE 7

Composition and Lattice Parameters of the Alloys Equilibrated at Various Temperatures

Aluminum A/o	Equilibrating Temp. °C	Lattice Parameter a Å	Lattice Parameter c Å	c/a
5.242	700	3.21696	5.12185	1.59214
-"-	600	3.22307	5.14236	1.59549
-"-	500	3.22972	5.14461	1.59289

From figure 7, the extrapolated value of "a" for pure zirconium (h.c.p.) is 3.2332 Å which is in close agreement with the reported value 3.2326 Å [5].

The value of "c" also initially decreases with aluminum content but increases in the range 1.24-3 A/o aluminum and then decreases again up to the solubility limit. This abnormal decrease and then increase of the "c" values could possibly be attributed to the overlap of the third or fourth Brillouin zones in the c direction

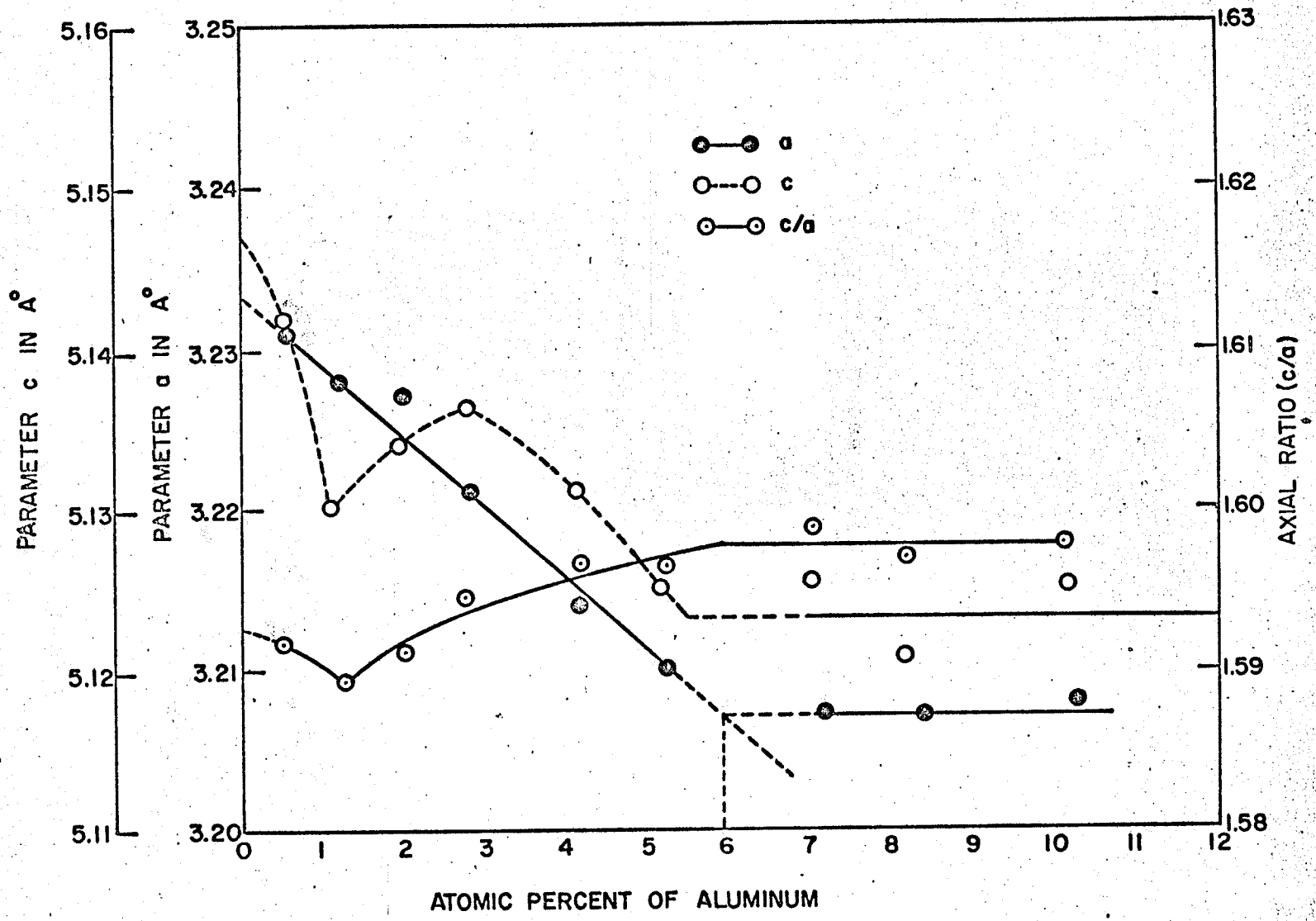

FIGURE 7 Lattice parameter/composition relations in the zirconium–aluminum alloys equilibrated at 850° C

(second Brillouin zone contains two electrons per atom). Jones[6a] has shown that overlap produces expansion of the lattice in the same direction as that of the overlap. The postulated overlap based on break at 1.24 A/o Al takes place at e/a = 3.987 (Zr-tetravalent, Al-trivalent).

Since "a" varies linearly with composition the c/a ratio, based on the "c" and "a" values from their respective curves in figure 7, shows the same abnormality at 1.24 A/o Al. In the two phase region c/a ratio is constant because "c" and "a" are constant.

3.3.2 Solid Solubility Values and the Solvus Curve

The solid solubility of aluminum in alpha zirconium at 850°C, as determined by the inflection point in the "a" versus composition curve in figure 7, is 5.95 A/o which is in close agreement with the previous[2] result, 5.8 A/o.

In figure 7, the compositions corresponding to the lattice parameters "a" of the alpha of the alloys equilibrated at 700, 600 and 500°C are respectively the solid solubility limits at those temperatures. The results are given in table 8.

TABLE 8

Solid Solubility Limits of Aluminum in Alpha Zirconium

Serial No.	Temp. °C	Al A/o
1	850	5.95
2	700	3.70
3	600	2.35
4	500	0.80

The solvus curve drawn on the basis of the above values is shown in figure 9, (heavy line).

"In many systems where a solid solution is in equilibrium with a phase of fixed composition, a straight line is obtained by plotting log S against $1/T^{o}K$, where S is A/o of solute at the limit of the solid solution. This relation does not have a conclusive thermodynamic basis, but is sufficiently general for any marked deviation to be taken as a strong hint that the solubility curve is in error"[7].

The curve between log S and $1/T^{o}K$ from the first five values of table 9 is shown in figure 8. The points lie very close to a straight line indicating that there is no serious error in the solubility values. Maximum solid solubilities at temperatures lower than $500^{o}C$ were determined by extrapolating the curve. These values are given in table 9. The solvus curve drawn down to temperatures lower than $700^{o}C$ is shown in figure 9, (heavy line to $500^{o}C$ and dotted line below $500^{o}C$).

It is seen that the solubility limits at temperatures lower than $850^{o}C$ determined in the earlier investigation[2] (based on metallographic methods) are much lower than found in the present work. The lower limits in the previous work[2] could be possibly due to incomplete homogenization. Due to the same possibility, the alloys reported as being in the two-phase region might have appeared to be so, though in fact they were in the single-phase region.

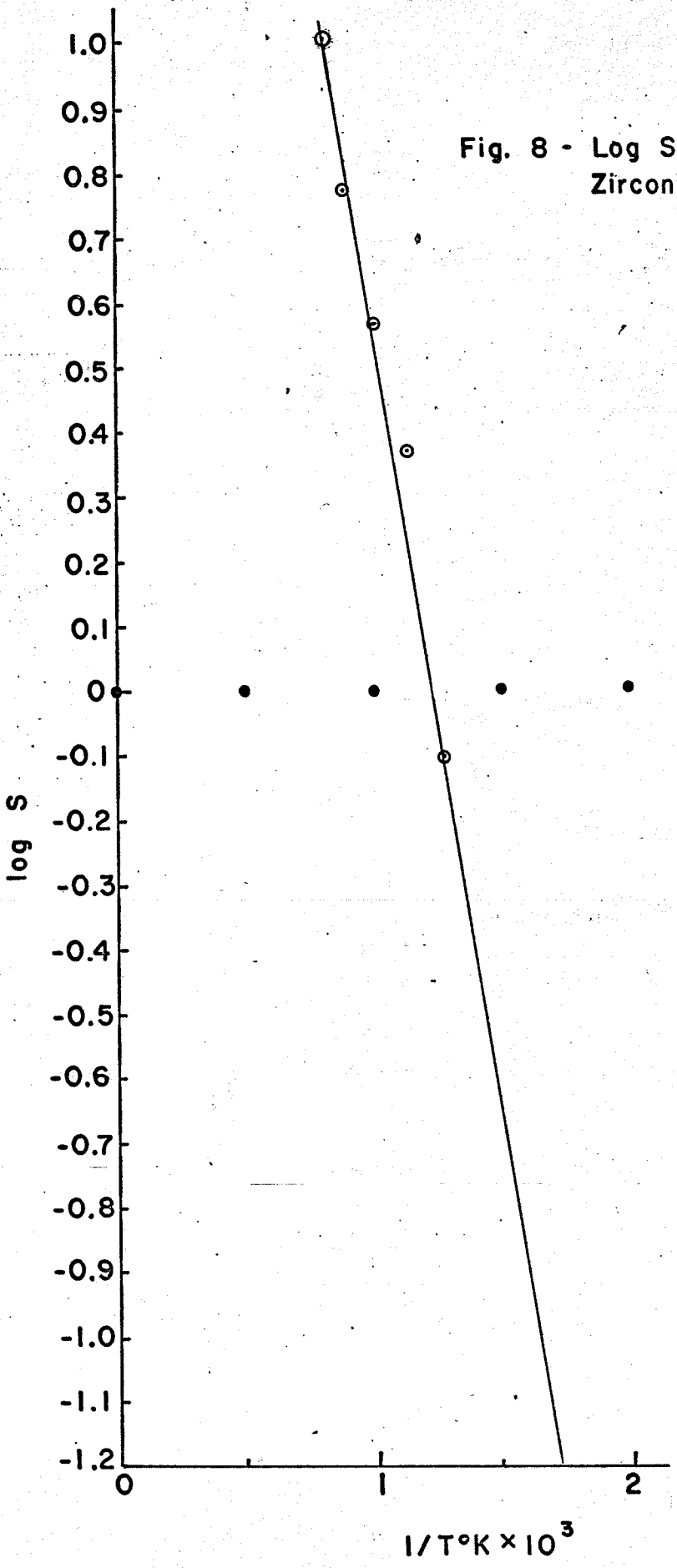

Fig. 8 - Log S V $\frac{1}{T°K}$ Curve for the Zirconium-Aluminum System

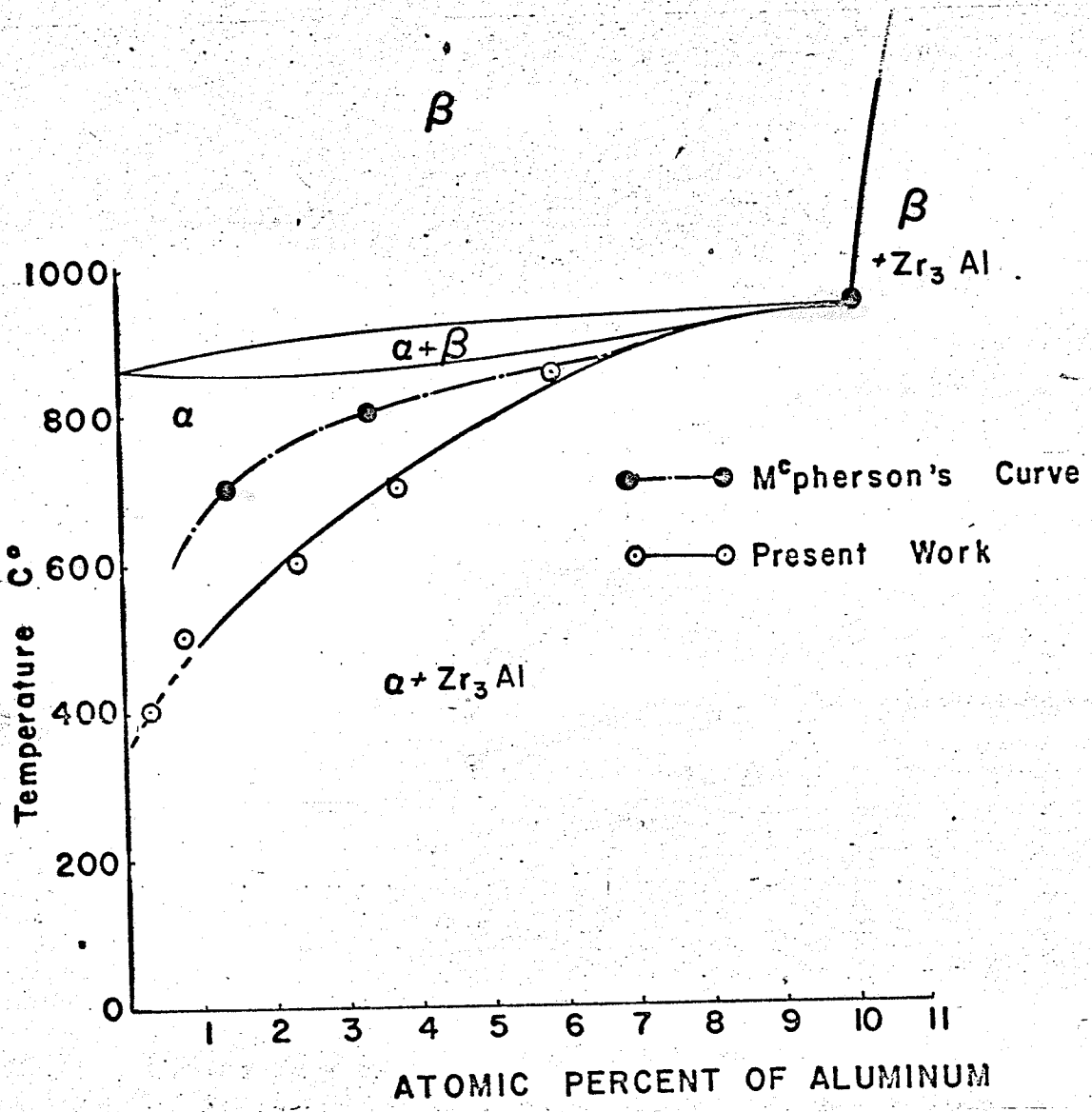

Fig. 9 - Solvus Curve in the Zirconium - Aluminum System.

TABLE 9

Solid Solubility Limits of Aluminum in Alpha Zirconium at Various Temperatures

Serial No.	Temp. ^{o}C	$1/T^{o}K$	Solid Solubility S A/o	Log S	Remarks
1	940	0.00082	$\sim$ 10	1.0	Published result (2)
2	850	0.00089	5.95	0.7745	Found experimentally
3	700	0.00102	3.70	0.5682	-"-
4	600	0.00114	2.35	0.3711	-"-
5	500	0.00128	0.80	0.9031	-"-
6	400	0.00148	0.31	$\bar{1}$.4900	Extrapolated value
7	300	0.00174	0.069	$\bar{2}$.8400	-"-
8	200	0.00211	$\sim$ 0.001	$\bar{2}$.1000	-"-
9	100	0.00268	very small	--	-"-
10	Room Temp.	0.00333	-"-	--	-"-

3.3.3 Metallographic Results and the Hardness Values (Supporting Evidence)

Photomicrographs of the equilibrated alloys (120 hours at $850^{o}C$ are numbered in the increasing order of aluminum content. Photos 1 to 6 show only one phase while photo 7, 8 and 9 show precipitate. The alloy in photo 7 has 7.128 A/o aluminum, i.e. beyond the solid solubility limit at $850^{o}C$. This result is consistent with the x-ray result.

The number of phases present in the alloys are given in table 10, the hardness values of these alloys are also shown. The

curve between the hardness (VPN) and the aluminum content, figure 10, also shows that the hardness increases in the single phase (alpha) region but remains almost constant in the two-phase (α + Zr_3Al) region.

TABLE 10

Metallographic Results and the Hardness Values of the Equilibrated ($850^{o}C$) Alloys

Sample No.	Al W/o	Al A/o	Phase(s) Present	VPN (1KG)
1	0.165	0.555	One	96 ± 3
2	0.370	1.240	One	103 ± 2.5
3	0.593	1.976	One	113 ± 3
4	0.845	2.800	One	114 ± 3
5	1.270	4.167	One	203 ± 7
6	1.610	5.242	One	218 ± 15
7	2.220	7.128	Two	250 ± 8
8	2.610	8.308	Two	250 ± 11
9	3.250	10.198	Two	241 ± 5

Photomicrographs 7, 8 and 9 show a pearlitic structure. Pearlitic precipitation was noticed by Keeler[8] also in alloys with more than 10 A/o aluminum which were treated near the transformation temperature. In the present case the alloys with 7.128, 8.3 and 10.2 A/o aluminum were held at $1000^{o}C$ (β region) for 5 hours and then cooled in the furnace to $850^{o}C$, held for 120 hours and then water quenched. When the alloys were furnace cooled from $1000^{o}C$ (β region)

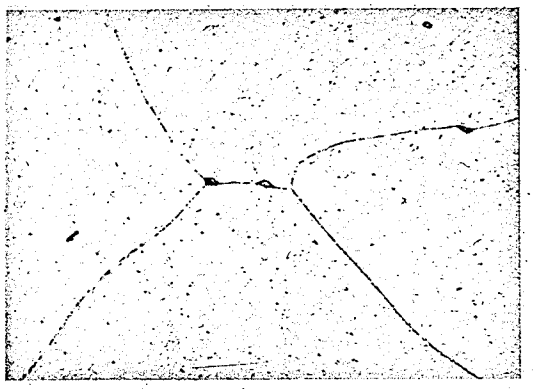

1. 0.55 A/o Al

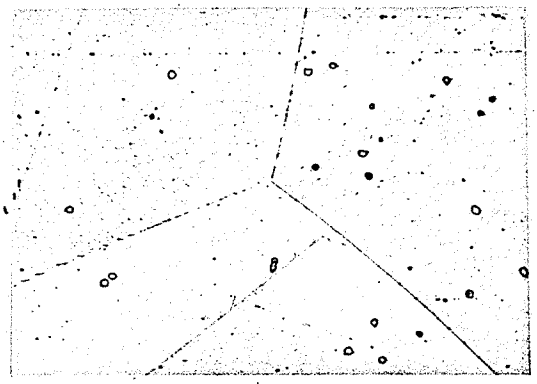

2. 1.24 A/o Al

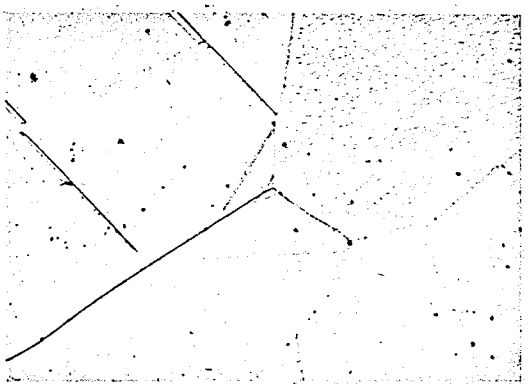

3. 1.98 A/o Al

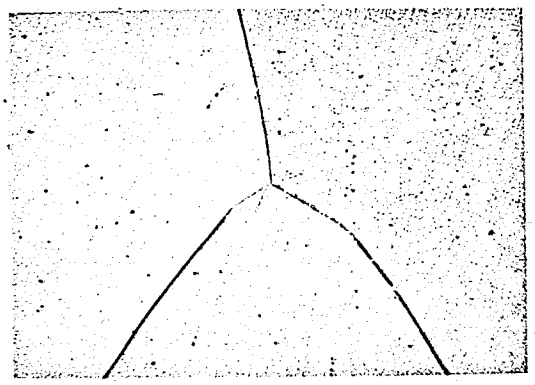

4. 2.8 A/o Al

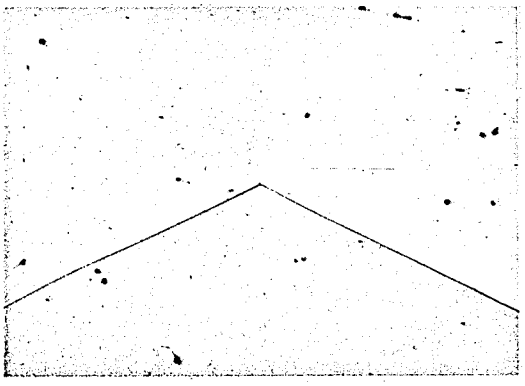

5. 4.167 A/o Al

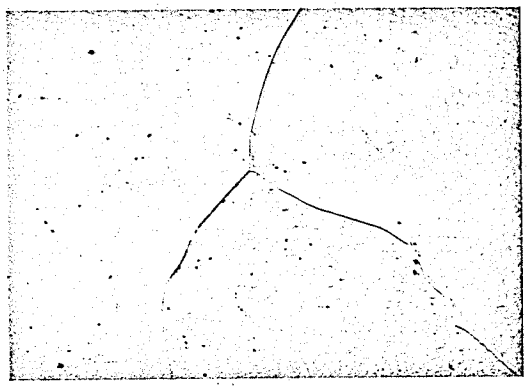

6. 5.242 A/o Al

Photo. 1-6 - Zr-Al alloys equilibrated at 850°C for 120 hrs. and then water quenched. All are single-phase. X 250.

7. 7.128 A/o Al

8. 8.308 A/o Al

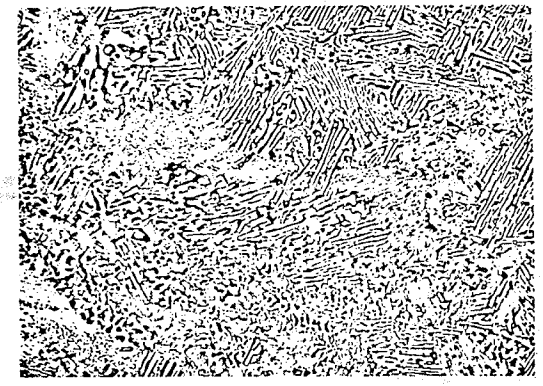

9. 10.198 A/o Al

Photo. 7-9- Zr-Al alloys equilibrated at 850°C for 120 hrs. and then water quenched. All are two phase. X250.

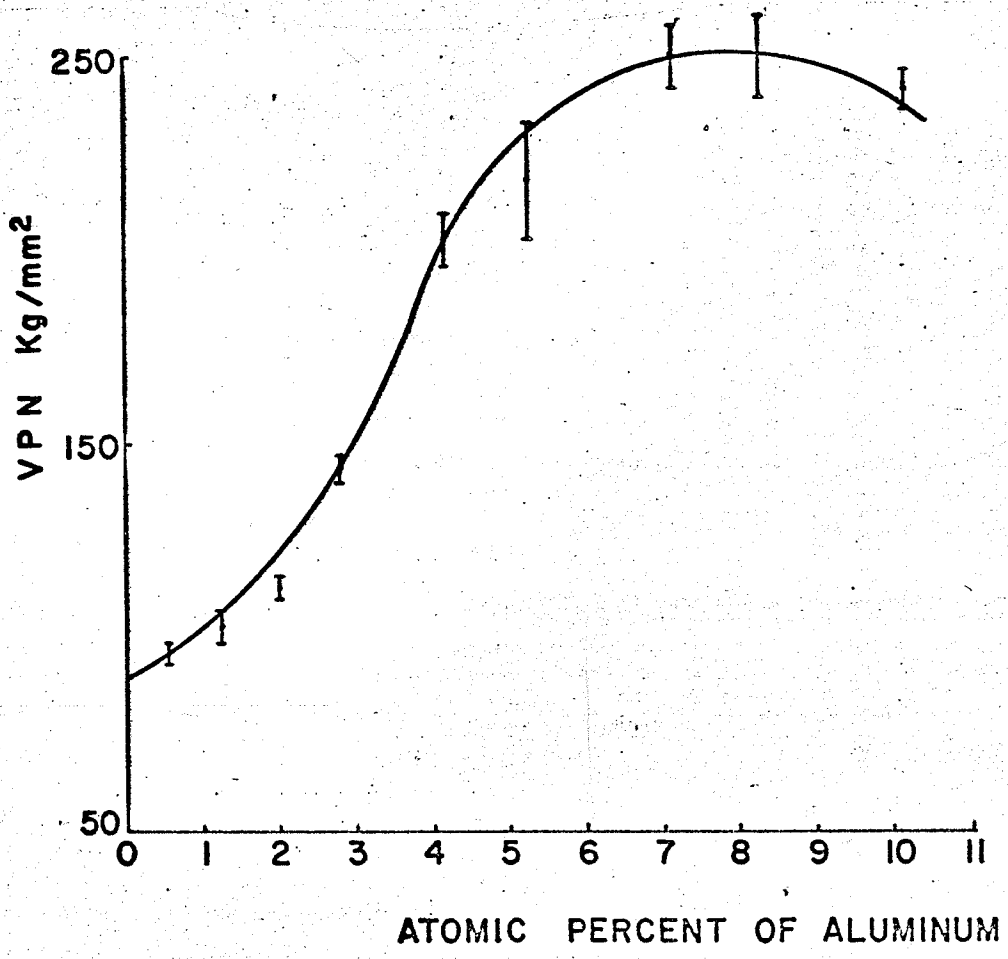

Fig. 10 – Hardness V Composition for the Zirconium-Aluminum Solid Solutions.

the time taken in passing through the ($\alpha + \beta$) and α regions might be very small and practically no phase-transformation from β to α phase could occur. Therefore, the alloys were nearly single phase and had β structure when cooled to 850°C. This β transformed to a completely pearlitic structure in the case of the 10.2 A/o aluminum alloy. These observations suggest that β phase decomposes into a pearlitic type structure composed of alternate layers of Zr_3Al and alpha zirconium.

The results obtained may be summarized as below - (for alloys equilibrated at 850°C).

Method \ Al A/o	0.55 1.24 1.976 2.8 4.167 5.242	7.128 8.308 10.198
X-Ray	Parameter "a" decreases	"a" remains constant
Metallography	Single phase	Two-phase
Hardness	Increases	Remains almost constant

4 STRENGTHENING EFFECT OF ALUMINUM ON ALPHA ZIRCONIUM

Results and Discussion

No systematic investigation of the solution hardening effect of aluminum on alpha zirconium has been made. There are incidental reports available on the strengthening effect of aluminum on zirconium but they are not really comparable due to the different metallurgical history of the specimens[9,10] and a lack of uniform test conditions. Therefore, it is difficult to correlate the results of various investigations. However, the curves between yield strength and composition are drawn in fig. 11, based on the results of previous works[1,9,10]. The curves based on the results of the present investigation (solution hardening effect) are also shown in fig. 11. The melting methods and heat treatment given in the earlier, as well as present investigation, are given in table 11.

TABLE 11

Melting Methods and Heat Treatments in Various Investigations

Investigator Reference	Melting Method	Heat Treatments of the Samples	Remarks
Anderson et al 9	High purity sponge melted in the atmosphere	As cast	Contained C up to 0.14%
Schowpe et al 10	Induction melted in graphite crucibles in vacuum	Cold rolled and annealed at 700°C for 1-3 hours	Contained ∿ 0.3% C
Keeler 1		Cold rolled and annealed at 800°C for one hour	
Present work	Argon-arc melted	Homogenized at 850°C for 120 hours and water-quenched	Reactor grade Zr was used

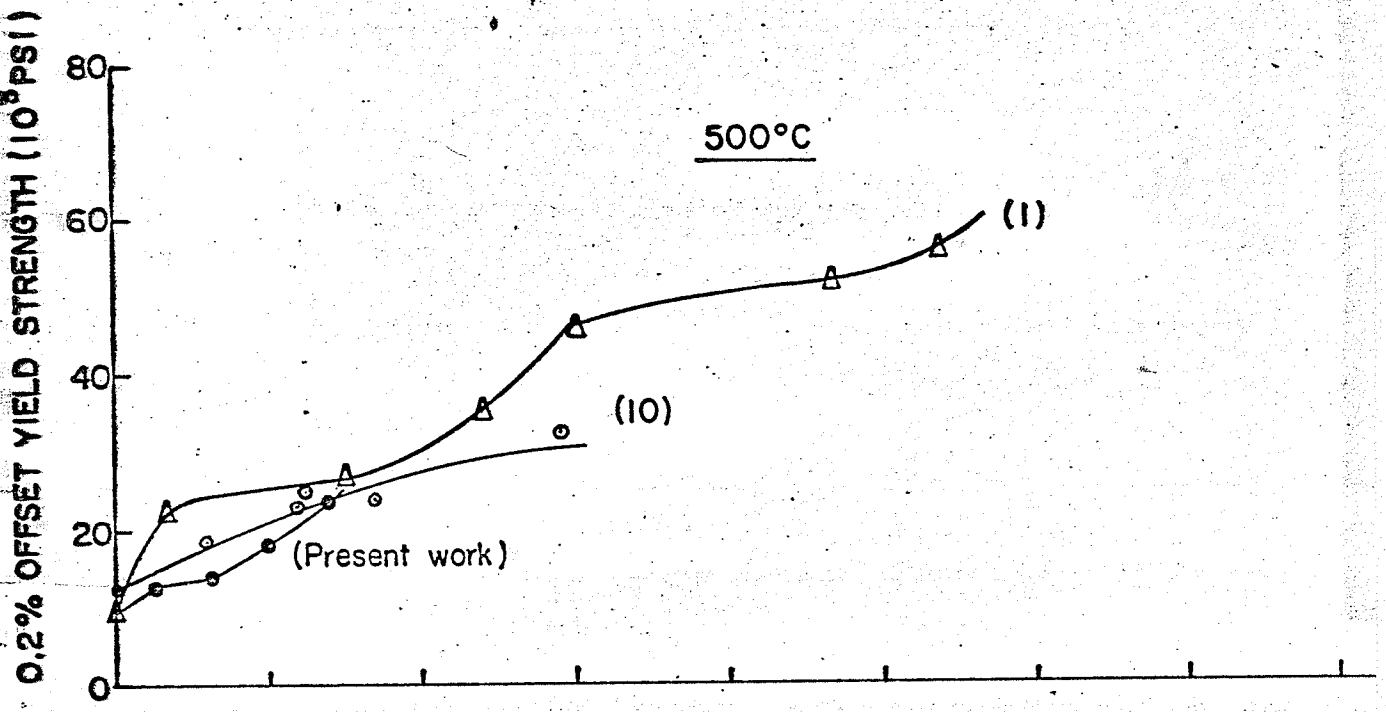

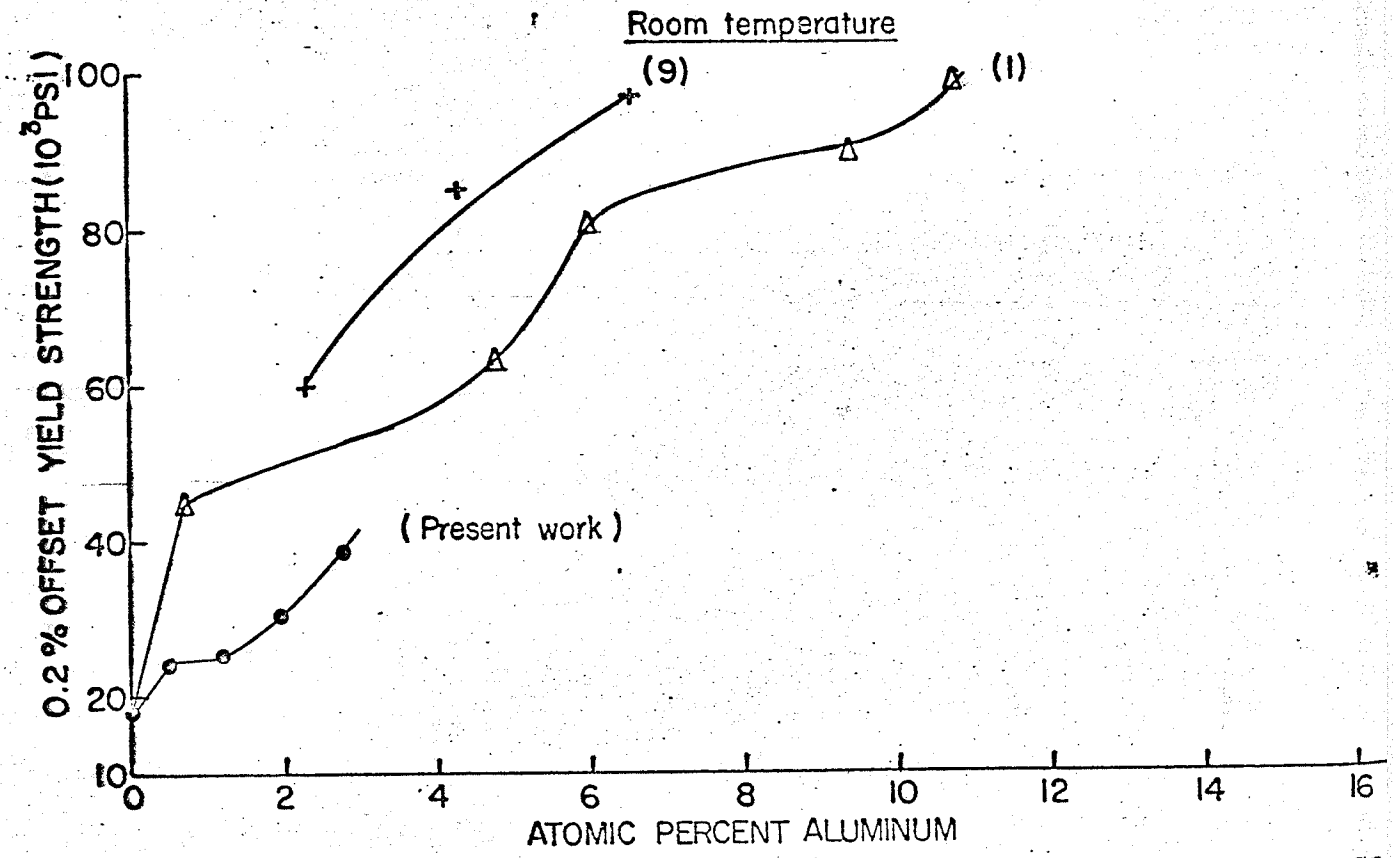

Fig. 11 – Relationship between yield strength and aluminum content at room temp. an
500°C

Results of Tensile Tests at Various Temperatures

Sample No.	Test Temp. °C	Al W/o	Al A/o	Yield Strength 0.2% offset 10^3 psi	Ultimate Tensile Strength 10^3 psi	Elongation %
1	Room (20°C)	Pure Zr		17.00	39.00	26.0
2		0.161	0.542	24.15	32.834	17.5
3		0.370	1.240	24.76	38.51	17.5
4		0.593	1.976	29.53	44.02	17.5
5		0.838	2.777	38.20	53.40	20.0
6	300	Pure Zr		10.00	18.00	27.0
7		0.161	0.542	16.36	20.34	23.0
8		0.370	1.240	15.10	21.32	24.0
9		0.593	1.976	21.46	26.33	15.0
10		0.838	2.777	26.64	34.89	20.0
11	500	Pure Zr		8.9	13.30	52.0
12		0.161	0.542	12.38	15.19	13.0
13		0.370	1.240	13.76	17.57	15.0
14		0.593	1.976	17.34	21.91	16.0
15		0.838	2.777	23.61	30.42	17.0

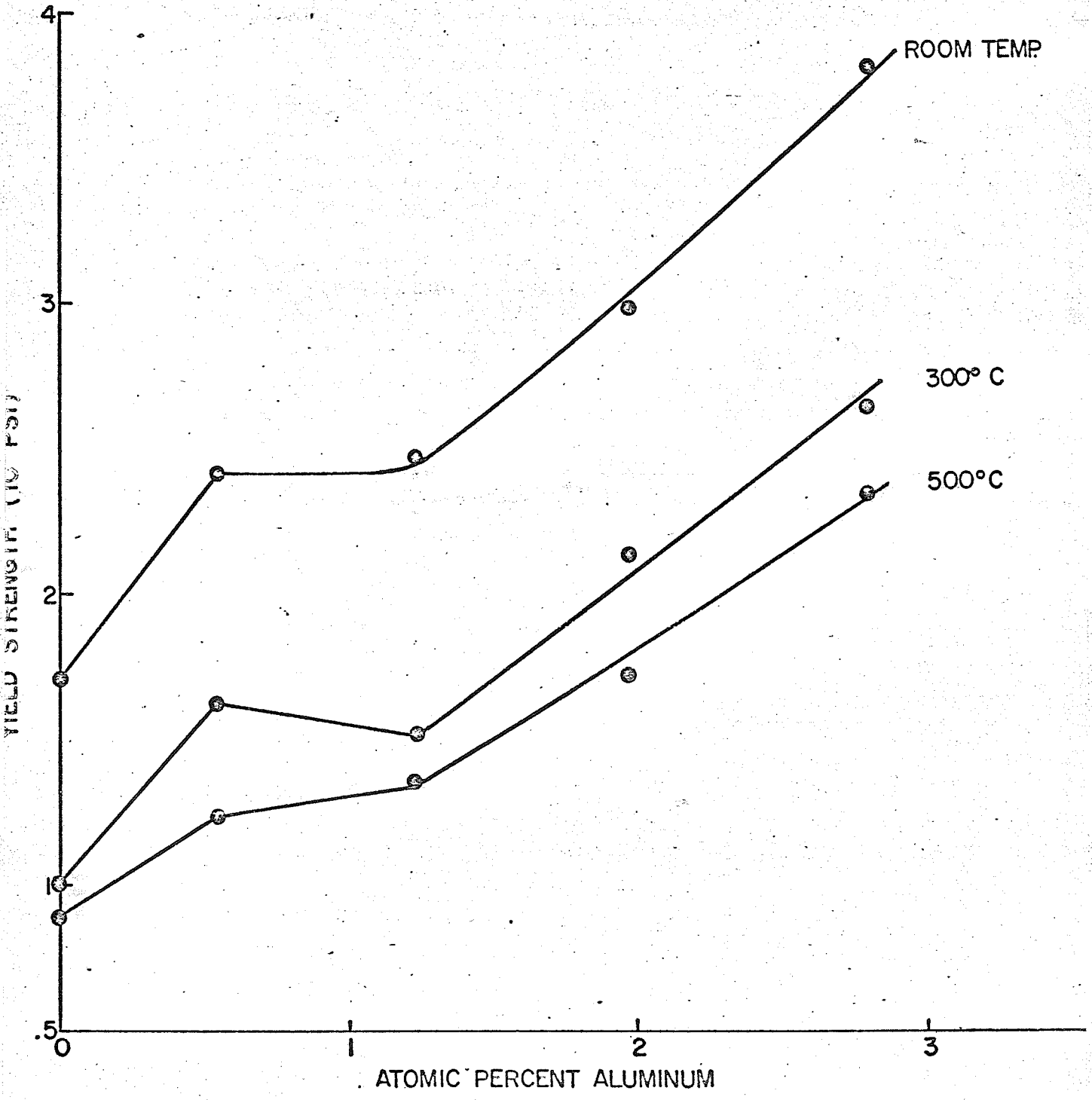

Fig. 12 – Yield strength versus composition for the zirconium-aluminum solid solutions

Because it was difficult to draw smooth curves through the points (four for each test temperature) and secondly, in the case of the curve without a knee the yield strength value for the lowest aluminum content alloy i.e. 0.542 A/o, will be very much lower than the observed yield strength in each case the curves were drawn with a 'knee', fig. 12. This knee was noticed in the curves of an earlier work[1] also, fig. 11, but the composition range of the knee is different in the two investigations. At present the presence of a knee in the curves is not well understood. Probably it can be related to the observed variation in the c/a ratio with the increasing aluminum content, fig. 7, and the relative increase in the stress required for dislocation glide on the (0001) planes as compared with the glide on the $\{10\bar{1}0\}$ planes[13] with increase in impurity (aluminum). In h.c.p. structures having a c/a ratio lower than the ideal value, 1.63, the prismatic glide i.e. $\{10\bar{1}0\}$ is favoured to the basal glide. As the c/a ratio increases, the tendency for the basal glide increases. In the present case the increase in aluminum content will render two opposing effects - one is the increase in tendency for the basal glide through the increase in c/a ratio and the other is the increased restriction on basal glide with increasing aluminum content. It seems that in the composition range 0.542 to 1.24 A/o aluminum both these effects balance each other and practically no hardening effect is observed, giving rise to the presence of the 'knee'.

Further investigation with the electron microscope and a more detailed study of the effect of aluminum for the composition range 0.1-1.0 A/o may reveal the reason.

The yield strengths of the zirconium-aluminum solid solutions are lower than the values for the cast or annealed alloys, fig. 11. From the heat-treatments of the alloys[1,9,10] and on the basis of the solvus curve determined in the present work it seems that the alloys were two-phase at the time of the test in the earlier investigations[1,9,10]. Possibly, precipitation hardening took place in these alloys which is a more effective mode of strengthening than the solution hardening.

After the abnormal increase in the yield strength by the initial addition of aluminum the yield strength of the zirconium-aluminum solid solutions increase almost linearly with the aluminum content beyond the knee. The rate of increase in the yield strength with compositions beyond the knee is nearly the same in both the earlier[1] and the present work.

The yield strength versus temperature curves for the solid solutions are shown in fig. 13. The yield strength decreases with the increasing test temperature because thermal activation energy helps in yielding of the metals. The rate of decrease of the yield strength with the temperature is nearly the same for all the zirconium-aluminum solid solutions.

It was found that the yield strength of the alpha zirconium at 500^{o}C was raised nearly equal to its yield strength at room temperature by the addition of about one A/o aluminum. At the room temperature itself an addition of 2.77 A/o aluminum raised the yield strength to more than twice its value.

The true stress-true strain curves for the solid solution alloys tested during the present investigation, are shown in

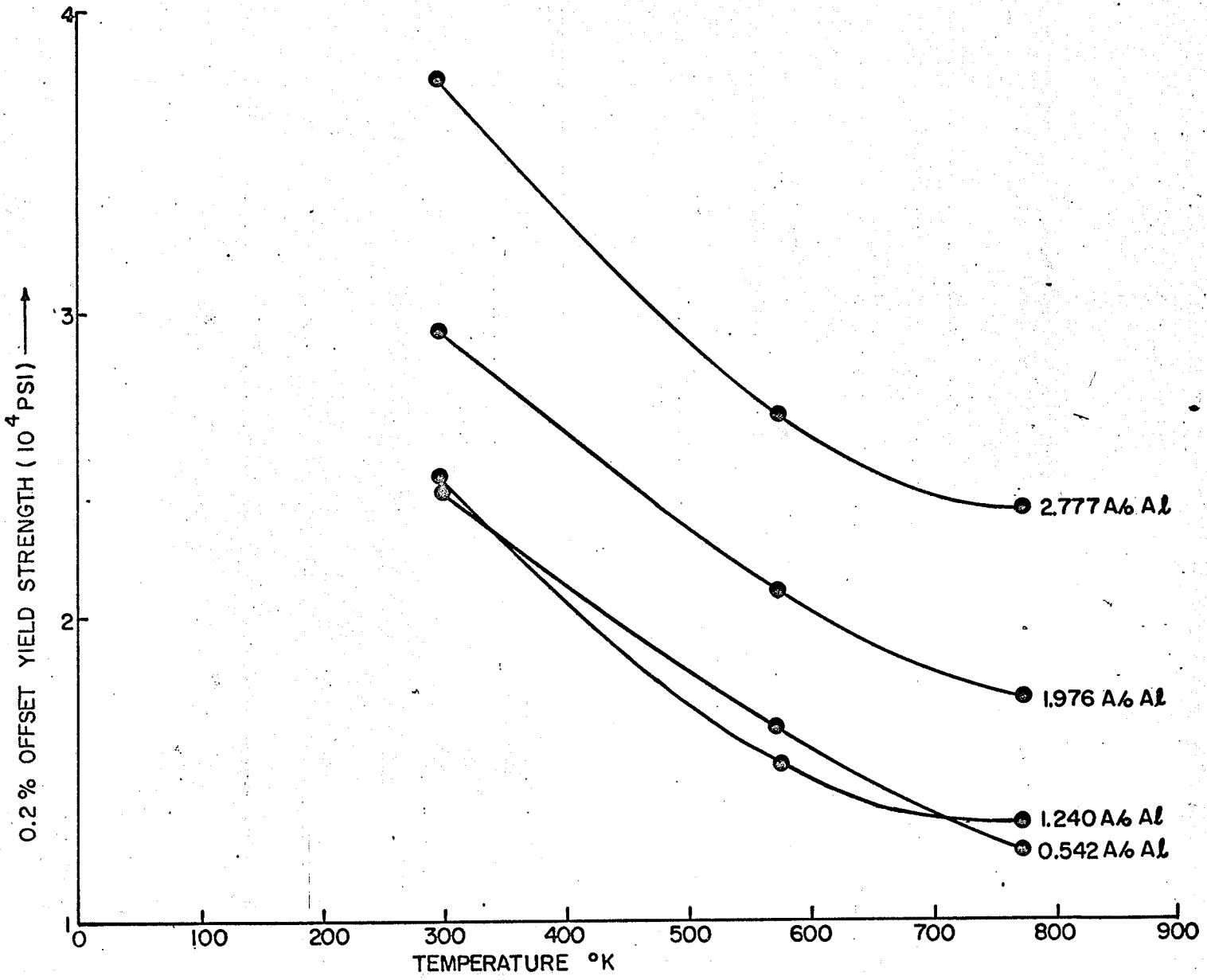

Fig. 13 – Yield strength versus test temperature for the zirconium – aluminum solid solutions

figs. 14, 15 and 16. It is seen that at all the test temperatures the slope of the linear portion of the curves i.e. Young's modulus (here qualitative in nature and not the absolute for the alloys tested), increases with the increase in aluminum content in the solid solutions. This may be due to the solvent-solute binding being stronger than the solvent-solvent. This conclusion is also indicated by the occurrence of numerous intermetallic compounds in the zirconium-aluminum system[2].

The slope in the parabolic region of the true stress-true strain curves, figs. 14, 15 and 16, indicates the work-hardening rate of the solid solutions at room temperature, 300°C and 500°C. At higher temperatures the thermal activation helps cross slipping which reduces the rate of work hardening. This is shown in figs. 17 and 18 by the decrease in the slope-angle, θ, (at 4% and 8% strain) with a rise in the testing temperature.

The slope in the parabolic region of the curves in figs. 14 or 15 or 16 increases with the increase in aluminum content, i.e. the work-hardening-rate increase.

The strengthening effect of aluminum on alpha zirconium may be the result of several factors. According to the Mott and Nabarro's[11] theory the frictional force due to the size-factor effect contributes towards the increase in the yield strength. But, in the present case due to the fact that the size misfit value is very small its contribution in raising the yield strength is expected to be rather small. Thus, it seems that the size-factor effect is not an important factor in the strengthening of alpha zirconium by aluminum.

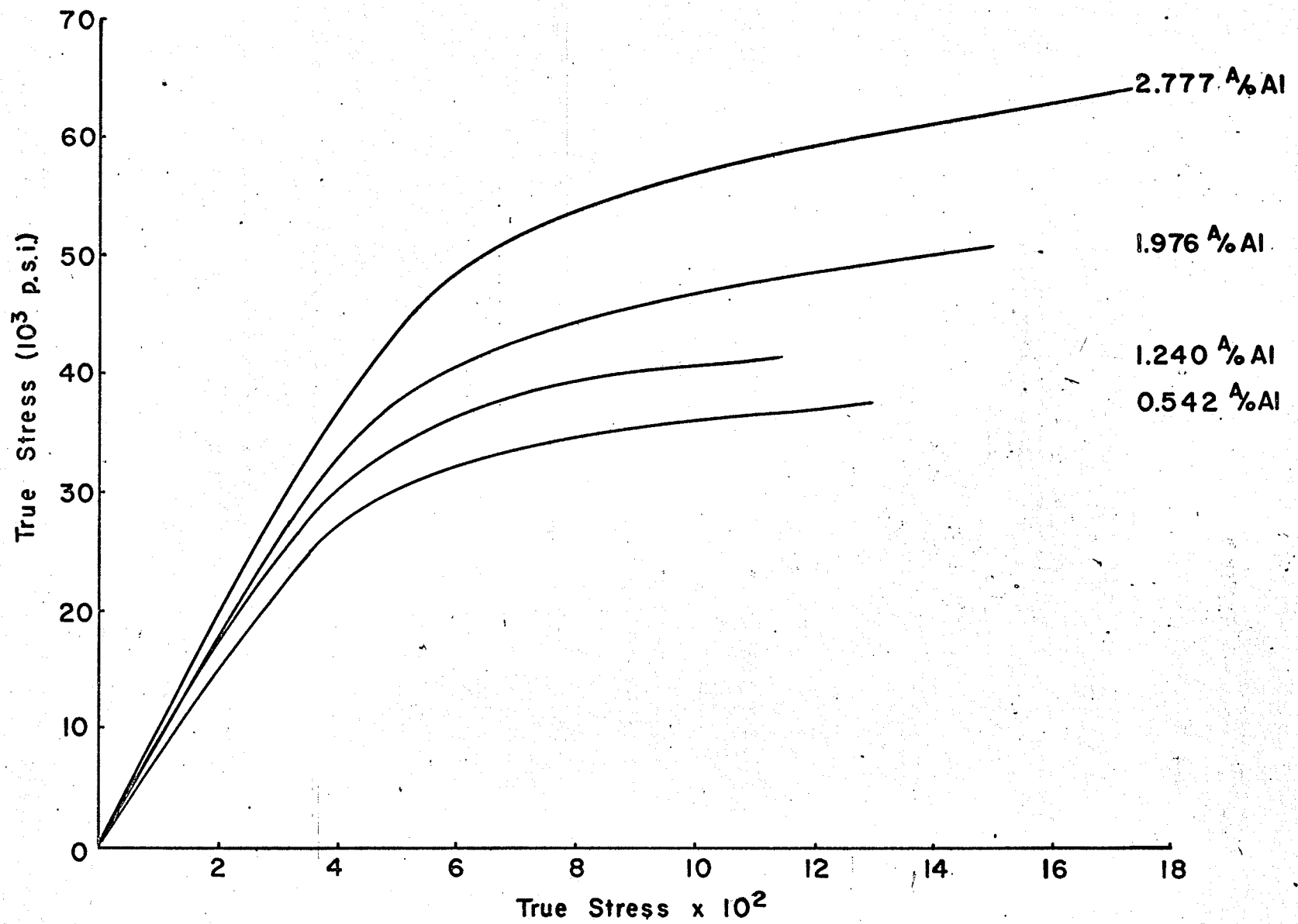

Fig. 14 - TENSILE TRUE STRESS - True Strain Curves for the Zirconium - Aluminum Solid Solutions at Room Temperature.

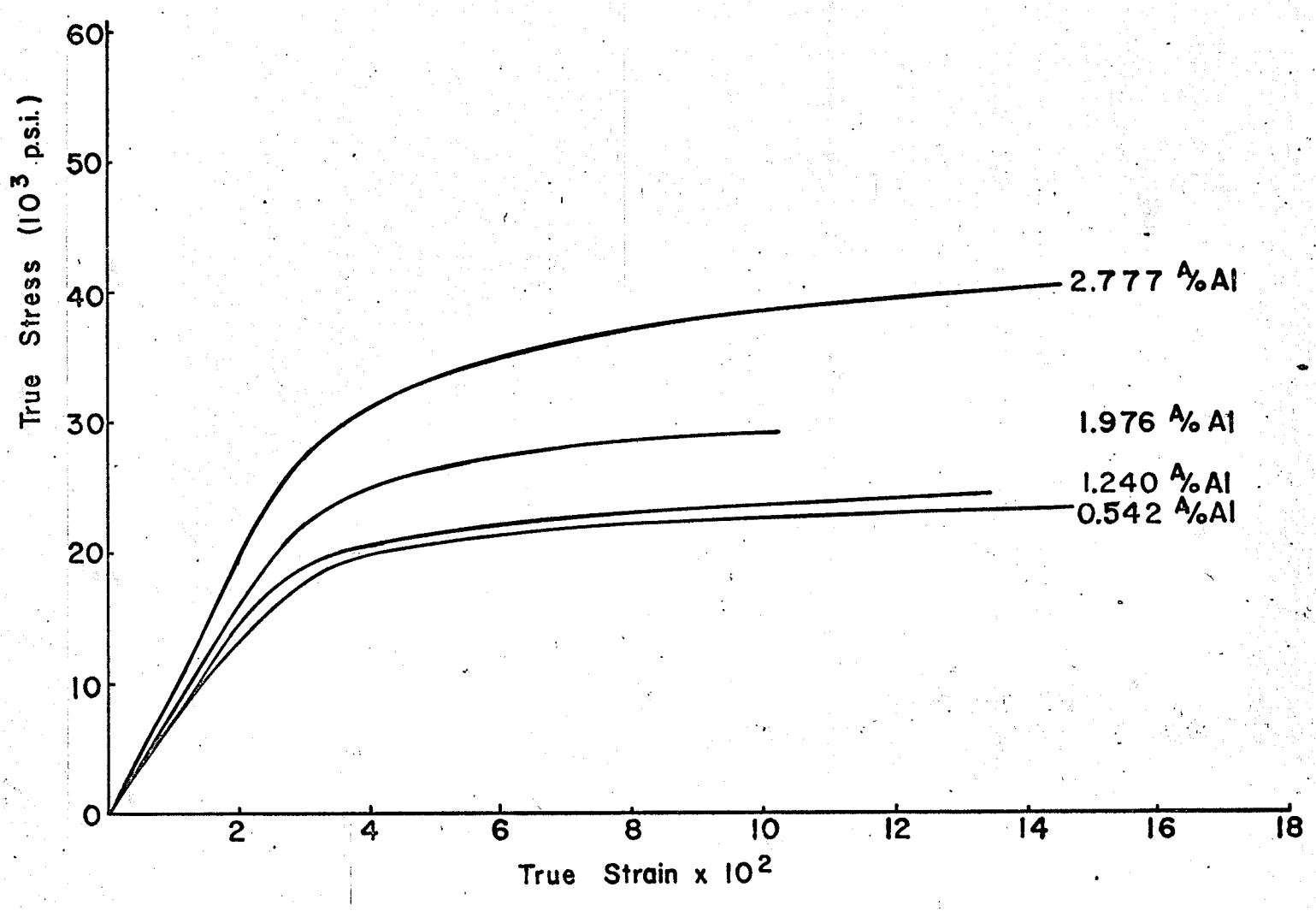

Fig. 15 - TENSILE TRUE STRESS - True Strain Curves for the Zirconium-Aluminum Solid Solution at 300° C.

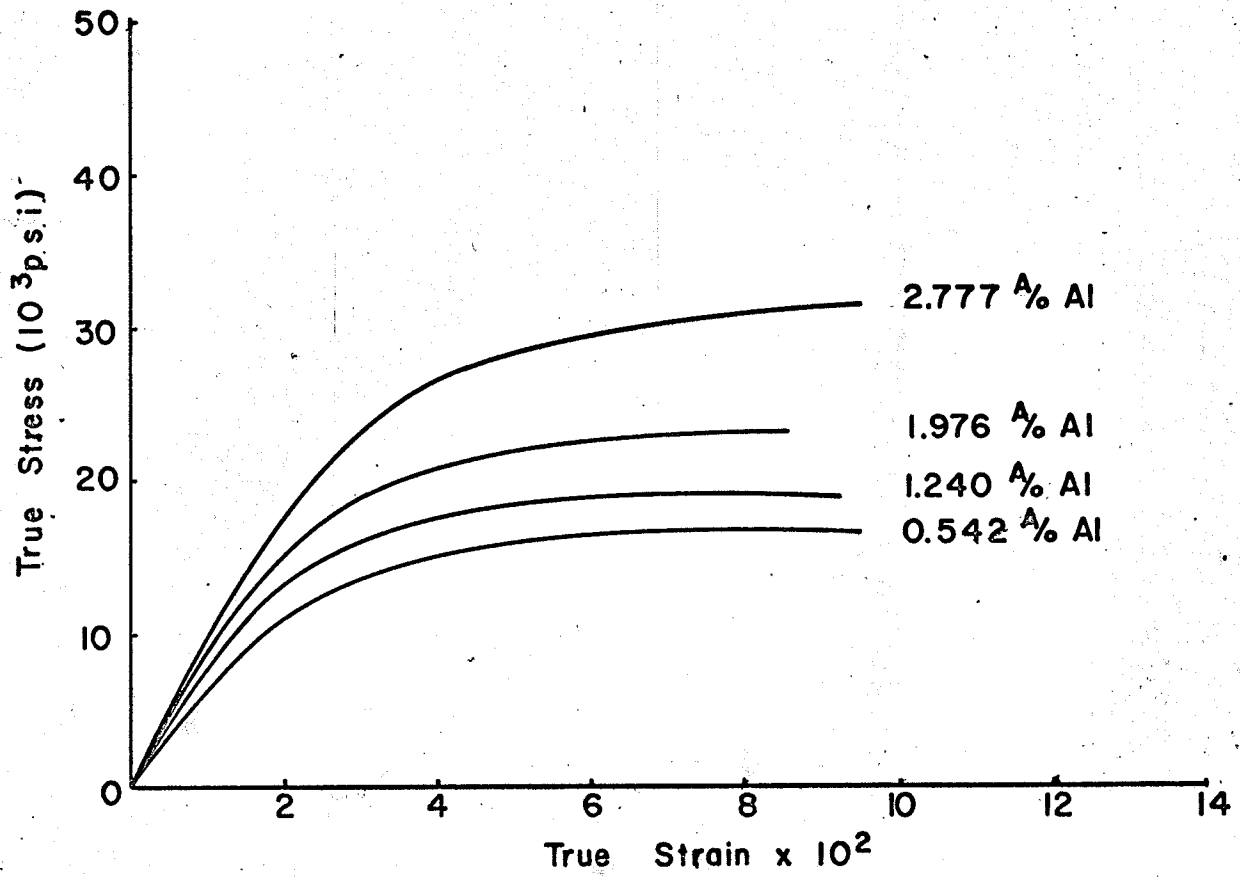

Fig. 16 — TENSILE TRUE STRESS - True Strain Curves for the Zirconium - Aluminum Solid Solutions at 500° C.

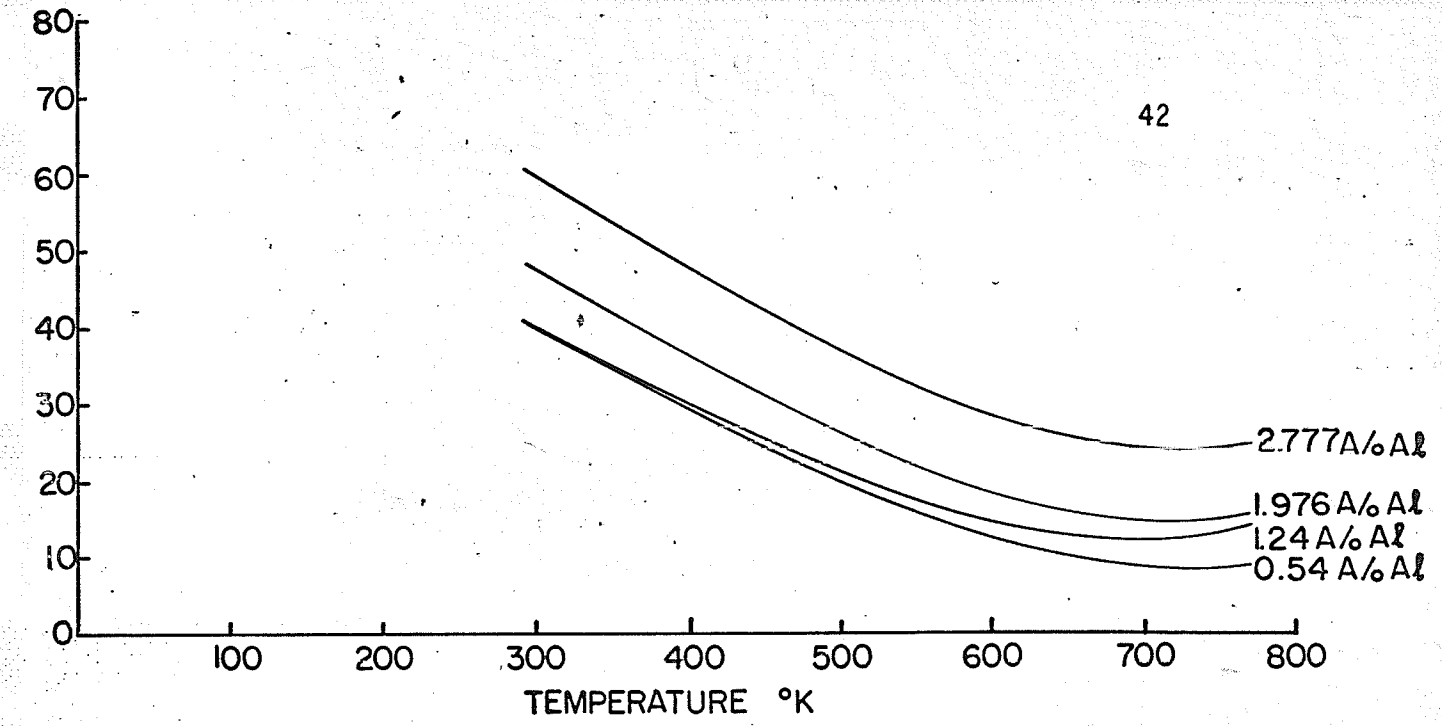

Fig. 17 – Slope angle θ at 4% strain vs temperature

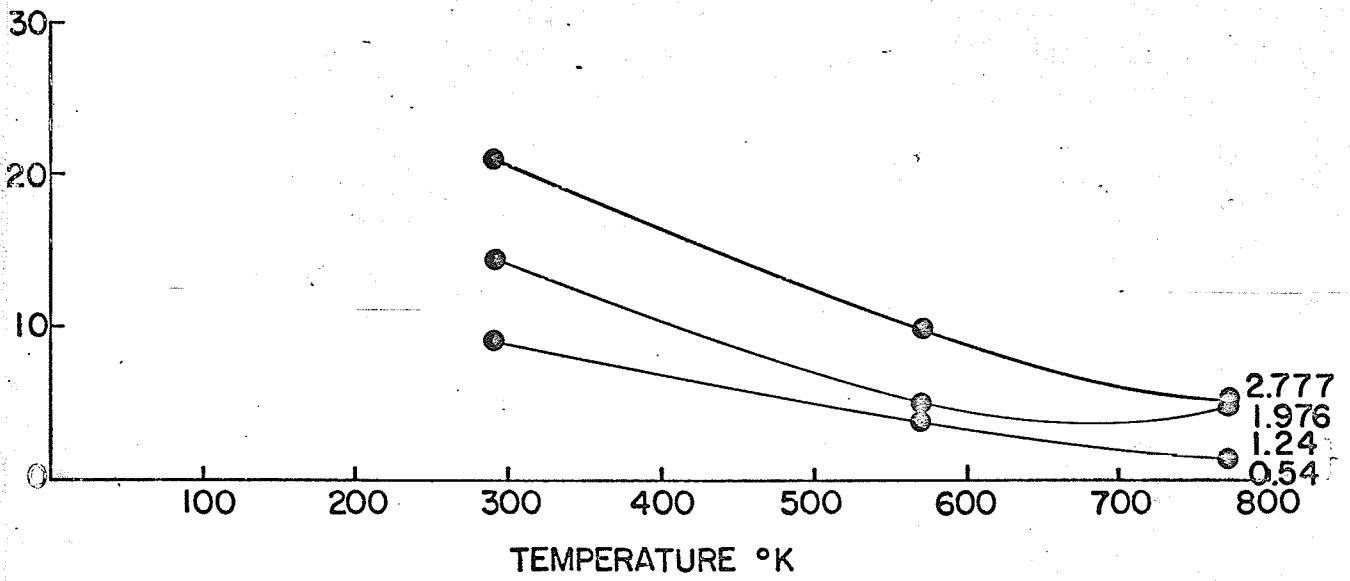

Fig. 18 – Slope angle θ at 8% strain vs temperature

Due to the absence of the value of modulus mismatch, the role of modulus effect (Fleischer's theory[12]) in increasing the yield strength could not be estimated. However, a rough estimation by using the change in hardness with composition (fig. 10) revealed that the predicted yield strength values are 5-10 times smaller than the observed ones.

On the basis of the observation that the solute-solvent bond is stronger than the solvent-solvent and the fact that numerous intermetallic compounds occur in the zirconium-aluminum system it seems that possibly short range ordering also has some contribution in the strengthening of alpha zirconium.

The critical resolved shear stress of single crystals is perhaps the only satisfactory parameter which can be used for a quantitative comparison with the theoretical predictions without any adjustable parameters (specially in the case of h.c.p. metals as they contain non-equivalent crystallographic planes). In the case of polycrystalline aggregates such adjustable parameters become important, because of the constraining conditions imposed by the grain boundaries.

However, the hardening effect of aluminum in the zirconium-aluminum solid solutions may be qualitatively explained on the basis of Bailey's[13] observations on the effect of impurities on the basal and prismatic slip in zirconium. However, further study of surface replicas and thin films by electron microscopy will be necessary to substantiate this hypothesis.

In zirconium the c/a ratio is lower than 1.633. Therefore, the interplaner spacing of the prism plans, $d_{\{10\bar{1}0\}}$ is more than the

the interplanar distance of the basal planes, $d_{(0001)}$, i.e. the ratio $d_{\{10\bar{1}0\}}/d_{(0001)}$ is more than unity, so that $\{10\bar{1}0\}$ have the lower Peierl's stress than the basal planes and are the favoured slip planes. The Burgers Vector is $\frac{1}{3}[11\bar{2}0]$ and $(10\bar{1}0)$ $[12\bar{1}0]$ is the predominant slip system[14]. Williams et.al.[15] have postulated that some basal slip is necessary to account for the observed texture in cold rolled zirconium. Bailey[13] has shown that in zirconium glide can occur on the basal plane at sufficiently high stress, e.g. around hydride precipitates or in the vicinity of triple points.

Thus it is seen that in zirconium the slip occurs on more than one set of crystallographically non-equivalent systems. As such, the solute dislocation interaction on different planes cannot be expected to be the same.

From studies on the changes in dislocation structure in deformed commercial and crystal bar zirconium Bailey[13] proposed that the stress for dislocation glide on $\{10\bar{1}0\}$ planes increases and glide on the basal planes becomes more difficult relative to glide on $\{10\bar{1}0\}$ with increasing impurity.

If it is assumed that the effect of aluminum on the prismatic and the basal glides is analogous to that of oxygen in zirconium the observed strengthening effect of aluminum may be explained as the sum of two effects. First, the dislocation glide on $\{10\bar{1}0\}$ planes (predominant slip planes) becomes difficult with increasing aluminum. Second, the motion of jogs is restricted which in turn impede the progress of both the edge and the screw dislocations. Jogs of dislocations on $\{10\bar{1}0\}$ planes lie in the basal planes, figs. 19 and 20.

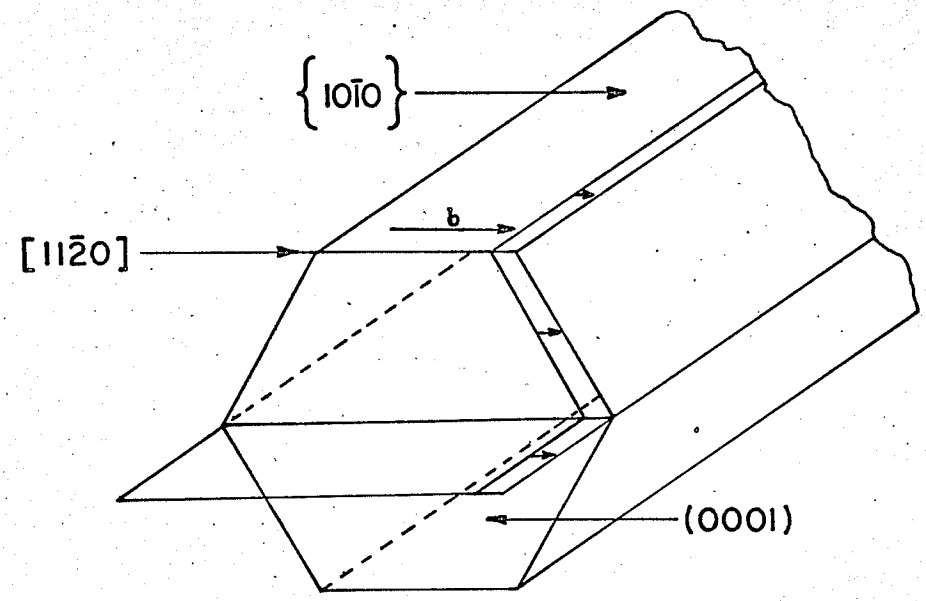

Fig. 19 Jog in the Edge Dislocation in α Zr

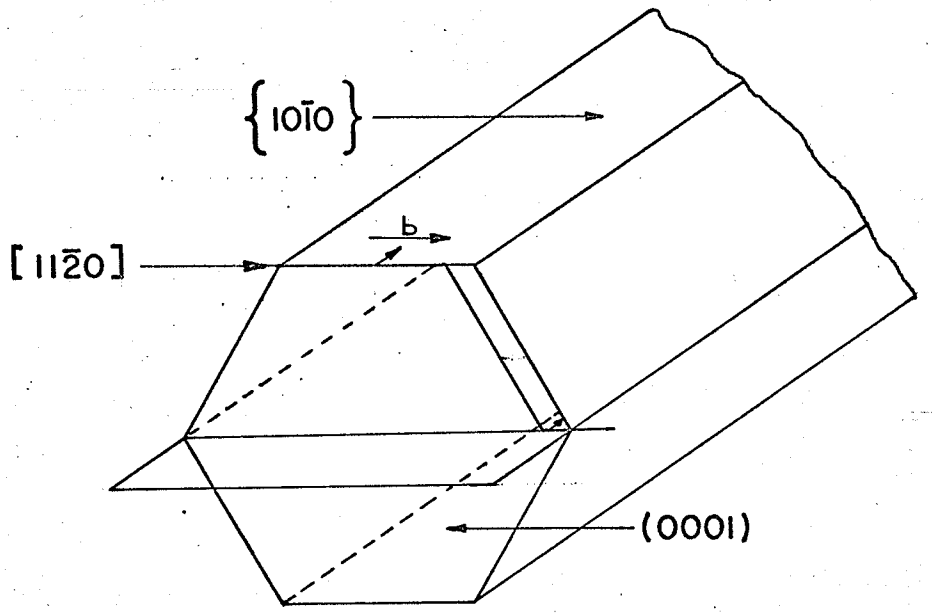

Fig. 20 Jog in the Screw Dislocations in α Zr

If slip is made more difficult on the basal planes then the possible basal glide of the jogs in edge dislocations is restricted. In the case of screw dislocations the jogs can move only non-conservatively which is more difficult since the advance of the dislocations requires the formation of point defects. Thus, the increased difficulty in the operation of basal glide, which is necessary for the general deformation, would cause considerable hardening of zirconium with increasing amount of aluminum.

The presence of stacking faults[16] on the basal plane in zirconium is evidence that the stacking fault energy is lowered by aluminum, photos 10 and 11. Due to this lowering of stacking fault energy extended jogs may form which would make a further contribution to the hardening of this system

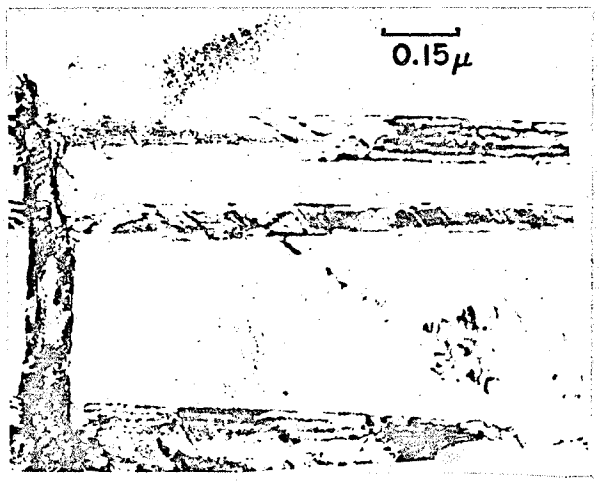

10. X 66000

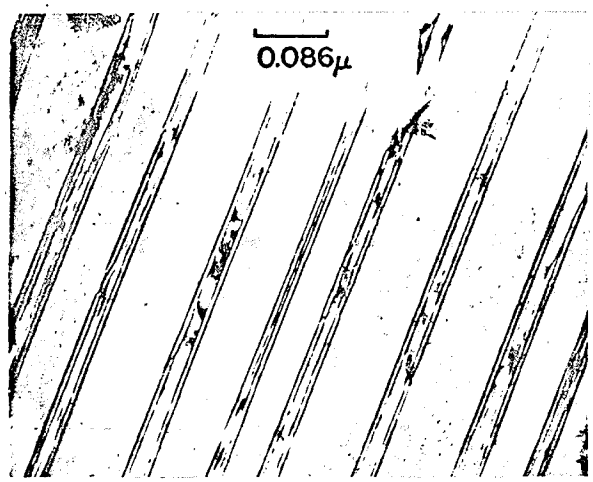

11 X 117000

Photo. 10 & 11 - stacking faults in Zr + 5.24 A/o Al alloy equilibrated at 1000°C (β region) for 5hrs and then water quenched.

5 CONCLUSIONS

1. Lattice parameter "a" of the zirconium-aluminum solid solutions changes by the relation

   $$a = 3.2332 - 0.0044x$$

   where x is aluminum in A/o.

2. Parameter "c" does not change regularly with aluminum additions.
3. An abnormal decrease in the value of "c" occurs at 1.24 A/o aluminum which may be attributed to the overlap of the Brillouin zones in the c direction.
4. The c/a ratio increases very slowly with the aluminum content.
5. The solid solubility of aluminum in alpha zirconium changes exponentially with the temperature like

   $$S = e^{-k/T^{o}K}$$

6. On cooling the β phase transforms to a pearlitic type structure.
7. The solid solubility of aluminum in alpha zirconium decreases very rapidly with the falling temperature and below 400°C it is very low.
8. Small amounts of aluminum raise considerably the strength of alpha zirconium at the room temperature as well as at the higher temperatures, in comparison to the room temperature strength of zirconium.
9. Solute-solvent bond seems to be stronger than the solvent-solvent.
10. The size misfit nor the modulus mismatch seem to be the controlling factor in the strengthening of zirconium by aluminum.
11. Possibly short range ordering has some contribution in the strengthening of alpha zirconium.

12. It is thought that the mechanism related to the different effects of aluminum on $\{10\bar{1}0\}$ and (0001) planes, is the important factor in the strengthening effect.

6 SUGGESTIONS FOR FUTURE WORK

1. Study of the effect of aluminum on the Brillouin zone of zirconium may explain the solid-solution and compound formation behaviour of the zirconium aluminum system.
2. Systematic study should be done to find the exact nature of decomposition on cooling of the β phase.
3. A detailed study of the zirconium-aluminum alloys in the composition range 0.1 → 1.0 A/o aluminum may explain the occurence of the knee in the yield strength versus composition curve.
4. An electron-microscopic-investigation of the deformation mode and the dislocation structure of the single crystals of zirconium-aluminum solid solutions may prove the hypothesis put forward in the present work.

7 REFERENCES

1. J.H. Keeler, G.E. Lab Report, Contract w-31-109-Eng-52, November, 1956.

2. D.J. McPherson and M. Hanson, Armour Research Foundation (00-89), April, 1952.

3. B.D. Cullity, Elements of X-Ray Diffraction, p. 338.

4. B.D. Cullity, Elements of X-Ray Diffraction, p. 354.

5. Swanson and Fuyat, NBS Circular 539, Vol. II (1953) 11.

6. Mott and Jones, 1937, Proc. Roy. Soc. A, 162, 49.

6a. H. Jones, 1934, Proc. Roy. Soc. A, 147, 400.

7. W. Hume Rothery, J.W. Christian and W.B. Pearson, Metallurgical Equilibrium Diagrams, p. 172.

8. J.H. Keeler, Trans. ASM 46 (1954), p. 373.

9. C.T. Anderson, 25 Zr Rich Alloy Systems, U.S. Bureau of Mines Report, 4658, March, 1950.

10. A.D. Schwope and W. Chubb, Journal of Metals, November, 1952, p. 1138.

11. N.F. Mott and F.R.N. Nabarro, Report on Conference on Strength of Solids, Phys. Soc. Land., p. 1.

12. R.L. Fleischer, Acta Met., 9 (1961) 996.

13. J.A. Bailey, Electron Microscope Studies of Dislocations in Deformed Zirconium, J. Nuc. Materials 7 (1962) 300.

14. E.J. Rapperport and C.S. Hartley, Deformation Modes of Zirconium at 77°, 575° and 1075°K-Trans AIME 218 (1960) 869.

15. D.N. Williams and D.S. Eppelsheimer, Origin of the Deformation Textures of Titanium, Nature 170 (1952) 146.

16. Z. Mishiyama et. al., Trans. Japan Inst. of Metals, Vol. 7, July, 1966.

APPENDIX

The difference between the observed and calculated values of the interplanar distance, d, for the zirconium-aluminum alloys are given below -

0.555 A/o Al - equilibrated at 850°C

hkl	Observed d (Å)	Calculated d (Å)	Difference Δd (10^{-3} Å)
100	2.7774	2.7981	20.7
002	2.5612	2.5780	16.8
101	2.4431	2.4577	14.6
102	1.8859	1.8932	7.3
110	1.6125	1.6155	3.3
103	1.4602	1.4616	1.4
200	1.3979	1.3990	1.1
112	1.3673	1.3678	0.5
201	1.3492	1.3499	0.8
004	1.2870	1.2855	1.5
202	1.2282	1.2287	0.5
104	1.1690	1.1681	0.9
203	1.0848	1.0838	1.0
210	1.0586	1.0576	1.0
211	1.0359	1.0359	0.0
114	1.0072	1.0059	1.3
212	0.9782	0.9781	0.1
105	0.9660	0.9653	0.7
204	0.9474	0.9466	0.8
300	0.9321	0.9327	0.6
213	0.9006	0.9000	0.6
302	0.8771	0.8768	0.3
205	0.8284	0.8287	0.3
106	0.8187	0.8194	0.7

1.24 A/o Al - equilibrated at 850°C

hkl	Observed d (Å)	Calculated d (Å)	Difference Δd (10^{-3} Å)
100	2.7907	2.7956	4.9
002	2.5654	2.5651	0.3
101	2.4534	2.4548	1.4
102	1.8902	1.8901	0.1
110	1.6143	1.6141	0.2
103	1.4603	1.4588	1.5
200	1.3965	1.3978	1.3
112	1.3669	1.3661	0.8
201	1.3488	1.3487	0.1
004	1.2867	1.2825	4.2
202	1.2293	1.2274	1.9
104	1.1694	1.1657	3.7
203	1.0847	1.0823	2.4
210	1.0572	1.0567	0.5
211	1.0354	1.0349	0.3
114	1.0064	1.0041	2.3
212	0.9783	0.9770	1.3
105	0.9655	0.9632	2.3
204	0.9478	0.9450	2.8
300	0.9321	0.9319	0.2
213	0.8997	0.8989	0.8
302	0.8764	0.8759	0.5
205	0.8291	0.8271	2.0
106	0.8160	0.8176	1.6

1.976 A/o Al - equilibrated at 850°C

hkl	Observed d (Å)	Calculated d (Å)	Difference Δd (10^{-3} Å)
100	2.7748	2.7949	20.1
002	2.5556	2.5670	11.4
101	2.4381	2.4548	16.7
102	1.8851	1.8906	5.5
110	1.6059	1.6137	7.8
103	1.4579	1.4595	1.6
200	1.3968	1.3975	0.7
112	1.3645	1.3662	1.7
201	1.3466	1.3484	1.8
004	1.2854	1.2835	1.9
202	1.2269	1.2274	0.5
104	1.1679	1.1664	1.5
203	1.0830	1.0824	0.6
210	1.0564	1.0564	0.0
211	1.0336	1.0347	1.1
114	1.0051	1.0045	0.6
212	0.9774	0.9769	0.5
105	0.9651	0.9638	1.3
204	0.9461	0.9453	0.8
300	0.9309	0.9316	0.7
213	0.8988	0.8989	0.1
302	0.8760	0.8758	0.2
205	0.8287	0.8275	1.2
106	0.8167	0.8182	1.5

2.799 A/o Al - equilibrated at 850°C

hkl	Observed d (Å)	Calculated d (Å)	Difference Δd. (10^{-3} Å)
100	2.7683	2.7834	15.1
002	2.5537	2.5655	11.8
101	2.4364	2.4466	10.2
102	1.8825	1.8864	3.9
110	1.6039	1.6070	3.1
103	1.4546	1.4572	2.6
200	1.3901	1.3917	1.6
112	1.3600	1.3619	1.9
201	1.3421	1.3432	1.1
004	1.2807	1.2828	2.1
202	1.2221	1.2233	1.2
104	1.1643	1.1650	0.7
203	1.0792	1.0795	0.3
210	1.0521	1.0520	0.1
211	1.0295	1.0306	1.1
114	1.0014	1.0025	1.1
212	0.9732	0.9734	0.2
105	0.9619	0.9629	1.0
205	0.9435	0.9432	0.3
300	0.9271	0.9278	0.7
213	0.8953	0.8961	0.8
302	0.8721	0.8725	0.4
006	0.8548	0.8552	0.4
205	0.8255	0.8259	0.4
106	0.8178	0.8175	0.3

4.167 A/o Al - equilibrated at 850°C

hkl	Observed d (Å)	Calculated d (Å)	Difference Δd (10^{-3} Å)
100	2.7663	2.7762	9.9
002	2.5520	2.5628	10.8
101	2.4349	2.4411	6.2
102	1.8798	1.8831	3.3
110	1.6008	1.6028	2.0
103	1.4531	1.4551	2.0
200	1.3888	1.3881	0.7
112	1.3579	1.3589	1.0
201	1.3393	1.3398	0.5
004	1.2812	1.2814	0.2
202	1.2212	1.2206	0.6
104	1.1629	1.1634	0.5
203	1.0767	1.0773	0.6
210	1.0498	1.0493	0.5
211	1.0274	1.0280	0.6
114	0.9995	1.0009	1.4
212	0.9704	0.9711	0.7
105	0.9606	0.9617	1.1
204	0.9414	0.9416	0.2
300	0.9258	0.9254	0.4
213	0.8933	0.8941	0.8
302	0.8707	0.8704	0.3
006	0.8544	0.8543	0.1
205	0.8242	0.8246	0.4
106	0.8171	0.8165	0.6

5.242 A/o Al - equilibrated at 850°C

hkl	Observed d (Å)	Calculated d (Å)	Difference Δd (10^{-3} Å)
100	2.7613	2.7770	15.7
002	2.5480	2.5608	12.8
101	2.4313	2.4412	9.9
102	1.8779	1.8826	4.7
110	1.6009	1.6033	2.4
103	1.4522	1.4544	2.2
200	1.3880	1.3885	0.5
112	1.3572	1.3589	1.7
201	1.3386	1.3401	1.5
004	1.2798	1.2804	0.6
202	1.2200	1.2206	0.6
104	1.1620	1.1628	0.8
203	1.0774	1.0772	0.2
210	1.0488	1.0496	0.8
211	1.0276	1.0282	0.6
114	1.0004	1.0005	0.1
212	0.9709	0.9712	0.3
105	0.9608	0.9610	0.2
204	0.9413	0.9413	0.0
300	0.9257	0.9257	0.0
213	0.8934	0.8941	0.7
302	0.8703	0.8705	0.2
006	0.8532	0.8536	0.4
205	0.8240	0.8243	0.3
106	0.8158	0.8159	0.1

7.128 A/o Al - equilibrated at 850°C

hkl	Observed d (Å)	Calculated d (Å)	Difference Δd (10^{-3} Å)
100	2.7722	2.7780	5.8
002	2.5571	2.5624	5.3
101	2.4396	2.4423	2.7
102	1.8827	1.8835	0.8
110	1.6029	1.6039	1.0
103	1.4548	1.4551	0.3
200	1.3876	1.3890	1.4
112	1.3594	1.3595	0.1
201	1.3407	1.3406	0.1
004	1.2795	1.2812	1.7
202	1.2217	1.2211	0.6
104	1.1628	1.1634	0.6
203	1.0771	1.0777	0.6
210	1.0507	1.0480	2.7
211	1.0282	1.0286	0.4
114	1.0009	1.0010	0.1
212	0.9708	0.9716	0.8
105	0.9612	0.9616	0.4
204	0.9417	0.9417	0.0
300	0.9258	0.9260	0.2
213	0.8938	0.8945	0.7
302	0.8704	0.8709	0.5
006	0.8534	0.8541	0.7
205	0.8246	0.8247	0.1
106	0.8166	0.8164	0.2

8.308 A/o Al - equilibrated at 850°C

hkl	Observed d (Å)	Calculated d (Å)	Difference Δd (10^{-3} Å)
100	2.7875	2.7896	2.1
002	2.5665	2.5682	1.7
101	2.4481	2.4514	3.3
102	1.8894	1.8894	0.0
110	1.6102	1.6106	0.4
103	1.4596	1.4592	0.4
200	1.3947	1.3948	0.1
112	1.3643	1.3645	0.2
201	1.3455	1.3461	0.6
004	1.2830	1.2841	1.1
202	1.2255	1.2257	0.2
104	1.1667	1.1665	0.2
203	1.0816	1.0814	0.2
210	1.0553	1.0544	0.9
211	1.0319	1.0328	0.9
114	1.0033	1.0041	0.8
212	0.9751	0.9754	0.3
105	0.9636	0.9640	0.4
205	0.9441	0.9447	0.6
300	0.9296	0.9299	0.3
213	0.8976	0.8978	0.2
302	0.8742	0.8743	0.1
006	0.8561	0.8561	0.0
205	0.8270	0.8272	0.2
106	0.8187	0.8184	0.3

10.198 A/o Al - equilibrated at 850°C

hkl	Observed d (Å)	Calculated d (Å)	Difference Δd (10^{-3} Å)
100	2.7587	2.7802	21.5
002	2.5422	2.5623	20.1
101	2.4260	2.4438	17.8
102	1.8765	1.8842	7.7
110	1.5997	1.6052	5.5
103	1.4513	1.4555	4.2
200	1.3872	1.3901	1.9
112	1.3580	1.3603	2.3
201	1.3394	1.3416	2.2
004	1.2783	1.2812	2.9
202	1.2200	1.2219	1.9
104	1.1625	1.1636	1.1
203	1.0773	1.0782	0.9
210	1.0503	1.0508	0.5
211	1.0275	1.0294	1.9
114	0.9995	1.0013	1.8
212	0.9710	0.9723	1.3
105	0.9603	0.9618	1.5
204	0.9410	0.9421	1.1
300	0.9259	0.0268	0.9
213	0.8940	0.8950	1.0
302	0.8710	0.8715	0.5
006	0.8541	0.8541	0.0
205	0.8246	0.8250	0.4
106	0.8159	0.8165	0.6

Zr-Al alloy equilibrated at 700°C

hkl	Observed d (Å)	Calculated d (Å)	Difference Δd (10^{-3} Å)
100	2.7679	2.7860	18.1
002	2.5532	2.5609	7.7
101	2.4359	2.4474	11.5
102	1.8818	1.8854	3.6
110	1.6045	1.6085	4.0
103	1.4550	1.4557	0.7
200	1.3913	1.3930	1.7
112	1.3611	1.3621	1.0
201	1.3424	1.3442	1.8
004	1.2816	1.2805	1.1
202	1.2229	1.2237	0.8
104	1.1655	1.1635	2.0
203	1.0796	1.0793	0.3
210	1.0517	1.0530	1.3
211	1.0302	1.0314	1.2
114	1.0020	1.0018	0.2
212	0.9750	0.9739	1.1
105	0.9626	0.9614	1.2
204	0.9431	0.9427	0.4
300	0.9277	0.9287	1.0
213	0.8863	0.8962	0.1
302	0.8736	0.8730	0.5
006	0.8546	0.8536	1.0
205	0.8265	0.8253	1.2
106	0.8159	0.8163	0.4

Zr-Al alloy equilibrated at 600°C

hkl	Observed d (Å)	Calculated d (Å)	Difference Δd (10^{-3} Å)
100	2.7646	2.7913	26.7
002	2.5470	2.5712	24.2
101	2.4303	2.4532	22.9
102	1.8788	1.8911	12.3
110	1.6038	1.6115	7.7
103	1.4544	1.4607	5.3
200	1.3909	1.3956	4.7
112	1.3589	1.3655	6.6
201	1.3411	1.3469	5.8
004	1.2813	1.2856	4.3
202	1.2226	1.2266	4.0
104	1.1647	1.1677	3.0
203	1.0786	1.0823	4.7
210	1.0525	1.0550	2.5
211	1.0302	1.0335	3.3
114	1.0020	1.0050	3.0
212	0.9743	0.9760	1.7
105	0.9638	0.9651	1.3
204	0.9440	0.9456	1.6
300	0.9290	0.9304	1.4
213	0.8974	0.8985	1.1
302	0.8737	0.8749	1.2
006	0.8558	0.8571	1.3
205	0.8269	0.8280	1.1
106	0.8192	0.8193	0.1

Zr-Al alloy equilibrated at 500°C

hkl	Observed d (Å)	Calculated d (Å)	Difference Δd (10^{-3} Å)
100	2.7699	2.7970	27.1
002	2.5546	2.5723	18.7
101	2.4370	2.4573	20.3
102	1.8800	1.8934	13.4
110	1.6054	1.6149	8.5
103	1.4545	1.4620	7.5
200	1.3890	1.3985	8.5
112	1.3614	1.3677	6.3
201	1.3427	1.3495	6.8
004	1.2833	1.2862	2.9
202	1.2249	1.2287	3.8
104	1.1661	1.1685	2.4
203	1.0813	1.0838	2.5
210	1.0536	1.0572	3.6
211	1.0325	1.0355	3.0
114	1.0037	1.0061	2.4
212	0.9761	0.9778	1.7
105	0.9622	0.9657	3.5
204	0.9488	0.9467	2.1
300	0.9327	0.9323	0.4
213	0.8983	0.8999	1.6
302	0.8745	0.8765	2.0
006	0.8550	0.8574	2.4
205	0.8272	0.8288	1.6